Synthesis, Characterization and Applications of Trinuclear Complexes with Schiff Base Ligands

M.Sc. Thesis

By **NITISH**



DISCIPLINE OF CHEMISTRY INDIAN INSTITUTE OF TECHNOLOGY INDORE JUNE 2019

Synthesis, Characterization and Applications of Trinuclear Complexes with Schiff Base Ligands

A THESIS

Submitted in partial fulfillment of the requirements for the award of the degree of

Master of Science

by NITISH



DISCIPLINE OF CHEMISTRY INDIAN INSTITUTE OF TECHNOLOGY INDORE JUNE 2019



INDIAN INSTITUTE OF TECHNOLOGY INDORE

CANDIDATE'S DECLARATION

I certify that the work which is being presented in the thesis entitled "Synthesis, Characterization and Applications of trinuclear complexes with Schiff Base Ligands" in the partial fulfillment of the requirements for the award of the degree of MASTER OF SCIENCE and submitted in the DISCIPLINE OF CHEMISTRY, Indian Institute of Technology Indore, is an authentic record of my own work carried out during the time period from July 2018 to June 2019 under the supervision of Prof. Suman Mukhopadhyay, Professor, IIT Indore.

The matter presented in this thesis has not been submitted by me for the award of any other degree of this or any other institute.

		NITISH
This is to certify that the correct to the best of my	e above statement mad	
	Prof. SUMA	AN MUKHOPADHYAY
NITISH has successful	ly given his M.Sc. Ora	l Examination held on
Signature of Supervisor Date:		Convener, DPGC Date:
Signature of PSPC member Date:	Signature of PSPC member Date:	Signature of PSPC member Date:



ACKNOWLEDGEMENTS

This is a lovely opportunity to offer thanks to all of the people who contributed from various perspectives to the successful completion of this thesis. I feel deep gratitude for all the people associated with my project work.

I would like to begin by thanking my supervisor Prof. Suman Mukhopadhyay, my PSPC committee members Dr. Amrendra Kumar Singh, Dr. Sampak Samanta and Dr. Tushar Kanti Mukherjee and DPGC convener Dr. Sanjay Kumar Singh for giving their constant support throughout the session.

I am hugely indebted to Prof. Suman Mukhopadhyay for his ceaseless encouragement and research guidance. I owe him for his support in terms of academics as well as on the emotional front. I also thank Prof. Pradeep Mathur and head of department Dr. Amrendra Kumar Singh for providing the necessary infrastructure and research support. The faculty members of the discipline of chemistry have also been very kind during the research period. I gratefully acknowledge them all for their consistent, supportive gesture. I would like to acknowledge SIC IIT Indore for giving instrumental supports.

All the results described in this thesis have been achieved with the help and support of lab partners and laboratory collaborators. Their friendly, collaborative behavior and realistic attitude have made this year a memory to be appreciated. I thank all my classmates for motivating me always during all the work of my project.

I also thank Mr. Ghanshyam Bhavsar, Mr. Kinney Pandey, Dr. Archana Chaudhary and Mr. Manish Kushwaha for assistance. And above all, I am forever obliged to my parents for giving me the experiences that have made me who I am. The motivation given by my parents was unconditional during execution of my project.

NITISH

Discipline of chemistry, IIT Indore

DEDICATED TO....

MY BELOVED FAMILY



Abstract

The present work of the thesis sums up the results of the findings on the synthesis, structural analyses, and spectral properties of some Schiff base complexes. Herein, three new trinuclear metal complexes from Schiff base ligand H_2L ($H_2L = 2,2'$ -((1E,1'E) -(propane-1,3diylbis(azaneylylidene))bis(methaneylylidene))diphenol) have been synthesized. Among them, one is a zinc Schiff base complex (1), and the remaining two are nickel Schiff base complexes (2 and 3) with 5substituted-1-H-tetrazole as a bridging ligand. All the complexes are characterized through ESI-MS, Elemental analyses and IR spectroscopy. Single crystal X-ray diffraction analyses have been done for all the three complexes 1, 2 and 3. Structural study reveals that the zinc (II) complex (1) is trinuclear and crystallizes in monoclinic system with space group P $2_1/c$ and both complexes 2 and 3 (nickel complexes) are trinuclear with triclinic crystal system and space group P- 1. Complex 1 has been found to be catalytically active in mimicking the functionalities of the metalloenzyme, phenoxazinone synthase (PHS). Interactions of complexes 2 and 3 with proteins (BSA and HSA) have been also studied to establish their potent role as metal-drug system.



TABLE OF CONTENTS

LIST OF FIGURES	xii
LIST OF TABLES	XV
NOMENCLATURE	xvi
ACRONYMS	xvii
Chapter 1: Introduction	1-8
1.1. General Introduction	1
1.2. Preparation and History of Schiff base and	4
tetrazoles	
1.3 Application of transition metal complexes	7
1.3.1 Metal complexes as biomimics	7
1.3.2 Metal complexes as protein	8
binding agents	
1.4 Organization of thesis	9
Chapter 2: Review of Past Work and Project	10-13
Motivation	
2.1 Biomimicking metalloenzyme	10
2.2 Biological applications	11
2.3 Magnetic properties	12
2.4 Gas adsorption	13
Chapter 3: Experimental Section	14-19
3.1 Reagents and Chemicals	14
3.2 Methods and Instrumentation	14
3.3 X-ray crystallography	14

3.4 Synthesis of Schiff-base Ligand and its metal	15
complexes	
3.4.1 Synthesis of Schiff base ligand (H ₂ L)	15
3.4.2 Synthesis of 5-phenyl-1- <i>H</i> -tetrazole	15
3.4.3 Synthesis of 5-(4-chlorophenyl)-1- <i>H</i> -tetrazole	16
$3.4.4$ Synthesis of $[Zn_3(L)_2(NO_3)_2]$	16
3.4.5 Synthesis of $[Ni_3(L)_2\{5-(4-chlorophenyl)-tetrazolato\}_2(DMF)_2]$	16
3.4.6 Synthesis of $[Ni_3(L)_2\{5\text{-phenyl} $ tetrazolato $\}_2(DMF)_2]$	17
3.5 BSA Binding study	17
3.6 HSA Binding study	18
3.7 Catalytic oxidation of 2-AP to 2-aminophenoxazinone	18
3.8 Detection of H ₂ O ₂ during the oxidation reaction	19
Chapter 4: Results and Discussion	20-50
4.1 Syntheses and Characterization	20
4.1.1 NMR spectra	24
4.1.2 Mass spectra	26
4.1.3 FT-IR spectra	28
4.3 BSA Binding study	
4.4 HSA Binding study	47

Chapter 5: Conclusion and Future Scope	51
REFERENCES	52-65

LIST OF FIGURES

Figure No.	Description	Page
Figure 1.1	Distinct coordination modes of substituted	3
	tetrazole ligand	
Figure 1.2	Catalytic activity of metalloenzyme	7
	phenoxazinone synthase	
Figure 1.3	3-D diagram of HSA and BSA	8
Figure 2.1	Spectra of APX band at around 434 nm,	10
	recorded after every 11 min intervals	
Figure 2.2	Fluorescence quenching by [NiL(5-	11
	phenyltetrazolato)] of BSA	
Figure 2.3	(a) Molecular structure of [Ni ₃ L ₂ (5-	12
	phenyltetrazolate) ₄ (DMF) ₂] (b) Molecular	
	structure of $[Ni_3L_2\{5-(3-pyridyl)\}]$	
	$tetrazolato\}_4 (DMF)_2] \cdot 2H2O$	
Figure 2.4	Molar susceptibility data were plotted for (a)	12
	and (b)	
Figure 2.5	(a) ORTEP diagram showing three Cadmium	13
	centers, (b) Displaying a 48-membered ring	
	having CdII cluster.	
Figure 2.6	Gas adsorption isotherms (for CO ₂ , green; for	13
	H_2 , black; for N_2 , red)	
Figure 4.1	¹ H NMR data of 5-phenyl-1- <i>H</i> -tetrazole ligand	24
Figure 4.2	¹ H NMR data of 5-(4-chlorophenyl)-1- <i>H</i> -	25
	tetrazole	
Figure 4.3	¹ H NMR data of Schiff base ligand H ₂ L	25
Figure 4.4	¹³ C NMR data of Schiff base ligand H ₂ L	26

Figure 4.5	HRMS of Schiff base ligand H ₂ L	26
Figure 4.6	HRMS of 5-phenyl-1- <i>H</i> -tetrazole	27
Figure 4.7	HRMS of 5-(4-chlorophenyl)-1- <i>H</i> -tetrazole.	27
Figure 4.8	ESI-MS of $[Zn_3(L)_2(NO_3)_2]$	27
Figure 4.9	IR spectrum of 1	28
Figure 4.10	IR spectrum of 2	28
Figure 4.11	IR spectrum of 3	29
Figure 4.12	Crystal diagram of [Zn ₃ (L) ₂ (NO ₃) ₂] showing	30
	atom numbering.	
Figure 4.13	Crystal structure of $[Ni_3(L)_2\{5-(4-$	33
	$chlorophenyl)\text{-}tetrazolato}_{2}(DMF)_{2}] showing$	
	atom numbering. Hydrogen atom are not	
	shown for clarity.	
Figure 4.14	$Crystal structure of [Ni_3(L)_2 \{ 5\text{-phenyl} \\$	36
	tetrazolato ₂ (DMF) ₂] showing atom	
	numbering. Hydrogen atom are not shown for	
	clarity.	
Figure 4.15	Spectra showing the growth of phenoxazinone	40
	species at 421 nm.	
Figure 4.16	Michaelis-Menten kinetics plot between rate of	40
	oxidation of 2-AP vs concentration of 2-AP	
	substrate in EtOH medium	
Figure 4.17	Plot between 1/r vs 1/s (Lineweaver-Burk plot)	40
Figure 4.18	ESI-MS spectrum recorded within 20 minutes	43
	of the oxidation reaction	
Figure 4.19	Characterized peak of I ₃ - for the qualitative	43
	detection of H ₂ O ₂ in 1 during the catalytic	
	oxidation process	

Figure 4.20	Fluorescence quenching of BSA by 2	44
Figure 4.21	Fluorescence quenching of BSA by 3	44
Figure 4.22	Stern -Volmer plot for 2	45
Figure 4.23	Stern-Volmer plot for 3	45
Figure 4.24	Scatchard plot for 2	46
Figure 4.25	Scatchard plot for 3	46
Figure 4.26	Fluorescence quenching of HSA by 2	47
Figure 4.27	Fluorescence quenching of HSA by 3	47
Figure 4.28	Stern-Volmer plot for 2	48
Figure 4.29	Stern-Volmer plot for 3	48
Figure 4.30	Scatchard plot for 2	49
Figure 4.31	Scatchard plot for 3	49

LIST OF TABLES

Table 4.1	Crystallographic refinement parameters for 1 3		
Table 4.2	Selected bond lengths (Å) for 1		
Table 4.3	Selected bond angles (°) for 1	32	
Table 4.4	Crystallographic refinement parameters for 2	34	
Table 4.5	Selected bond lengths (Å) for 2	34	
Table 4.6	Selected bond angles (°) for 2	35	
Table 4.7	Crystallographic refinement parameters for 3	37	
Table 4.8	Selected bond lengths (Å) for 3	37	
Table 4.9	Selected bond angles (°) for 3	38	
Table 4.10	Summary of kinetic parameters of	41	
	phenoxazinone synthase (PHS) mimicking the		
	activity of catalyst 1		
Table 4.11	Table showing the value of K_{sv} , K_q , K_a and n	50	

NOMENCLATURE

λ	Wavelength
θ	Angle
α	Alpha
β	Beta
γ	Gamma
Å	Angstrom
δ	Chemical shift (NMR)
ν	Frequency
°C	Degree Centigrade
\bar{v}	Wavenumber
cm	Centimeter
%	Percentage
g	gram
mol	mole
mmol	millimole
M	Molar
mM	millimolar
L	Litre
mL	mililitre
μL	microlitre
nm	nanometer
K	Kelvin
s	second

ACRONYMS

С	Carbon
0	Oxygen
Н	Hydrogen
N	Nitrogen
Zn	Zinc
Ni	Nickel
МеОН	Methanol
EtOH	Ethanol
DMF	Dimethylformamide
2-AP	2-aminophenol
APX	Phenoxazinone
TON	Turn Over Number
KI	Potassium Iodide
H_2SO_4	Sulfuric acid
H_2O_2	Hydrogen peroxide
HSA	Human Serum Albumin
BSA	Bovine Serum Albumin
Tris-HCl	Tris(hydroxymethyl)aminomethane-
	hydrochloride

HCl	Hydrochloric acid
KBr	Potassium Bromide
ORTEP	Oak Ridge Thermal Ellipsoid Plot Program
ESI-MS	Electron Spray Ionization- Mass Spectrometry
NMR	Nuclear Magnetic Resonance spectroscopy
UV-Vis/NIR	Ultraviolet-visible Near IR

Chapter 1

Introduction

1.1 General Introduction:

In 1913, Alfred Werner was given the Nobel prize in chemistry for his pioneering work on defining basics of coordination chemistry that explains the structure and bonding in coordination complexes [1]. The science concerned with the interaction of inorganic or organic ligands with metal centers has remained active research areas in Inorganic chemistry. A broad variety of stable coordination compounds or complexes can be formed by transition elements in which central atom is bonded to ligands through coordinate bonds [2]. The exploration for new metal coordination compounds is going on, not only for their interesting structural aspects but also for their emerging applications in the area of dyes, colors, nuclear fuels, photography, toxicology, medicine, ceramics, magnetic and catalytic materials [3-6] etc. The utilization of coordination compounds by nature and their mechanistic analysis has increased their popularity in chemistry as well as biology [7]. The central metal ion and the surrounding ligand influence the chemistry of transition metal complexes substantially [8]. The knowledge of the oxidation state and geometric preference of the transition metals in their complexes is essential for knowing the coordination chemistry of transition metal complexes. Furthermore, the electron donor properties of the ligands and their positions in coordination sphere can have a more significant influence on structures and functionality of metal coordination compounds [9,10].

Over the years, a great curiosity in synthesis and formulation of transition metal Schiff base complexes has been witnessed [11]. Biological activities of the complexes particularly with Schiff base ligands are profoundly investigated area due to their easy preparation,

versatility, different coordination behaviors and improved activities in contrast to non-Schiff base complexes [12-14]. N, O-containing donor ligands specifically the salen type "N₂O₂" donor symmetrical Schiff base ligands have drawn attention of the synthetic chemists presumably because of their synthetic simplicity and forming metal complexes effortlessly with the possibility of lots of applications. Polynuclear metal complexes containing such type of salen ligands have potential ability in mimicking certain enzymes or proteins which can ultimately act as the source of stimulation, storage and carrier of molecular oxygen in enzymatic routes e.g. galactose oxidase, cytochrome *c* oxidase, catechol oxidase, phenoxazinone synthase (PHS) [15-19] etc. Metal chelates formed from Schiff base ligands show wide variety of application in the medicinal field, catalysis reactions, anti-corrosion compounds and antibacterial properties [20,21].

Azole based moieties hold great importance due to the presence of nitrogen atom in them, which can act as a donor atom having the capability to bind with different metal centres. This interesting advantage can be efficaciously utilized in the field of catalysis, material science, biology [22] etc. Among the heterocyclic ligands; tetrazoles are known to gain importance due to their diverse coordinating ability to produce mono- as well as polynuclear complexes [23]. Swedish chemist Bladin had prepared the first Tetrazole complex in 1885. Tetrazoles are synthetic organic heterocyclic compound, comprising of five-membered rings of one C-atom and four nitrogen atoms [24]. Medicinal chemistry utilizes tetrazole containing motifs in the design of new drugs [25]. Tetrazoles possess similar acidity to carboxylic acids as it contains a dissociable N-H which is acidic in nature [26]. Henceforth, they can also act as a bio isosteres for carboxylate group [27]. Generally, all three nitrogen of tetrazoles is capable of acting as a coordinating site to form coordination compounds.

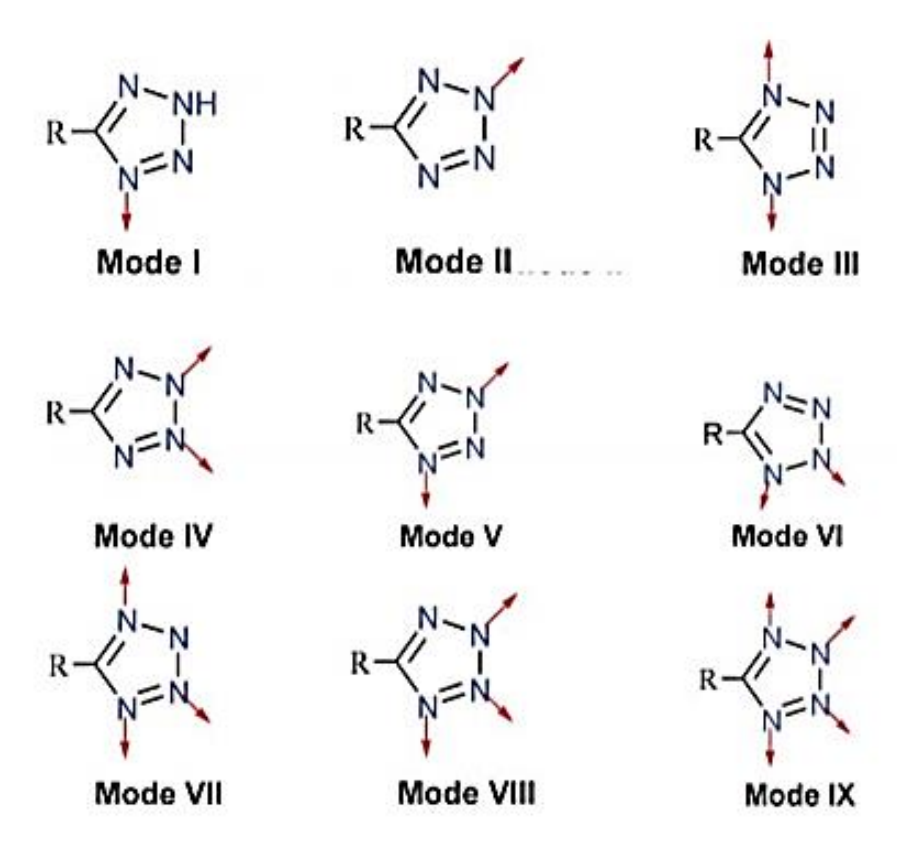


Figure 1.1: Distinct coordination modes of substituted tetrazole ligand

Scientists have been synthesizing, studying, and applying tetrazole compounds in various areas for more than 100 years now [28]. In recent years metal complexes of tetrazoles have gained much interest and have been explored due to their excellent capability and distinct coordination modes (Figure 1.1) to generate diverse coordination compounds with widespread applications in presence or absence of other bridging or capping ligands. Complexes of tetrazoles are mostly synthesized via solvothermal methods [29-31] and also it is known to form insoluble metal-organic frameworks with possible applicability in gas storage and capture [32,33], anti-corrosion species [34], adsorption [35], magnetic materials [36-39], photoluminescence [40,41], catalysis [42,43] etc. Over recent years [2 + 3] cycloadditions of metal ligated azides and nitriles are also being employed to synthesize metal tetrazole complexes [44-46]. The extra stability of the tetrazolato ligands is an added advantage for synthesizing such kind of complexes.

1.2 Preparation and History of Schiff base and tetrazoles

Schiff base is the compound with the general structure having the azomethine group (-HC=N-). Hugo Schiff reported the first Schiff base in 1864. Schiff base is the product from a 1° amine (aliphatic or aryl amine) and aldehydes or ketones by nucleophilic addition followed by removal of water to give an (-HC=N-) imine [47].

Generally, formation of Schiff bases takes place under basic or acidic condition or with heat.

$$R \longrightarrow NH_2$$
 + $R'' \longrightarrow R''$ $R'' \longrightarrow R''$

Scheme 1.1: Reaction scheme of Schiff base ligand preparation

Synthesis of Schiff base ligand is a reversible reaction, and its preparation gets completed by dehydration or formation of the product [48]. In this case, the amine is the nucleophile, and nucleophilic attack takes place at carbonyl compound to give unstable carbinolamine (addition compound). Generally, loss of water takes place from carbinolamine *via* acid or base catalyzed pathways. Being an alcohol carbinolamine go through acid catalyzed dehydration.

Scheme 1.2: Reaction Scheme showing the preparation of Schiff base through carbinolamine (unstable compound)

Tetrazoles are cyclic five-membered unsaturated aromatic heterocycles. Tetrazoles are not freely found in natural surroundings [49]. Fascinatingly, among all stable heterocycles tetrazole possess the highest number of nitrogen atoms because even at low temperature pentazoles are found to be highly explosive in nature [50]. The Swedish chemist J. A. Bladin obtained the first tetrazole derivative at the University of Upsala in 1885 [51]. It was found that the reaction between nitrous acid and dicyanophenylhydrazine gives a compound with the molecular formula $C_8H_5N_5$. Bladin named it "tetrazole" for the aromatic structure. Tetrazoles synthesis involves different solvents, but Demko and Sharpless have found a greener approach by employing the use of zinc salt in water in reflux conditions to furnish tetrazoles, which have proved to be quite a popular method [52].

$$R \longrightarrow C \longrightarrow N$$

$$R \longrightarrow N$$

$$N \longrightarrow N$$

Scheme 1.3: Schematic representation of Zinc bromide catalyzed the formation of tetrazoles

G. Vanketesh Verlag *et al.* reported CdCl₂ catalyzed formation of tetrazoles [53].

Scheme 1.4: Schematic representation of CdCl₂ catalyzed formation of Tetrazoles

Lakshmi Kantam *et al.* described ZnHAP catalyzed formation of tetrazoles from various types of nitriles and sodium azide [54].

(HAP= Hydroxyapatite)

Scheme 1.5: Schematic representation of ZnHAP catalyzed the synthesis of tetrazoles

David Amantini *et al.* proposed TBAF catalyzed formation of tetrazoles in the cycloaddition of nitriles with TMSN₃ under solvent less conditions [55]. (TMSN₃=Azidotrimethylsilane; TBAF=Tetra-n-butylammonium fluoride)

Scheme 1.6: Schematic representation of TBAF catalyzed cycloaddition of benzonitriles with TMSN₃ under solvent less conditions

Julien Bonnamour *et al.* used cheap and environmentally friendly [Fe(OAc)₂] as a catalyst to prepare substituted 5-*H*-tetrazoles in good yield [56].

$$R \longrightarrow C \longrightarrow N$$

$$[Fe(OAc)_2] (10 \text{ mol}\%)$$

$$DMF/MeOH$$

$$Reflux$$

$$R$$

Scheme 1.7: Schematic representation of Fe(OAc)₂ catalyzed synthesis of tetrazoles

1.3 Applications of Transition metal complexes:

1.3.1 Metal complexes as Biomimics:

Enzymatic catalysis has taken a lot of attention in this period as molecules which can mimic enzymes catalyze a variety of reactions with high selectivity and it can happen even under ordinary conditions [57]. Chemists today face challenges in the path to synthesize coordination compounds which can act as functional mimics of metalloenzymes. Such coordination compounds which have the capability of imitating the metalloenzyme can give insights into the mechanistic pathways of enzymes [58]. Oxidation reactions are of the utmost value in the industries as well as in the research laboratories [59,60]. Polynuclear transition metal Schiff base complexes have shown potential ability to mimic the enzymes by enticing certain metalloproteins which can ultimately act as the source of stimulation and carrier of molecular oxygen in enzymatic routes e.g. cytochrome c oxidase, galactose oxidase, catechol oxidase, phenoxazinone synthase (PHS) [61,62] etc. Phenoxazinone synthase (PHS) is the multicopper oxidase which can catalyze the formation of o-quinone imine from o-aminophenol and the successive coupling of o-aminophenol and o-quinone imine furnishes phenoxazinone [63].

Figure 1.2: Catalytic activity of metalloenzyme phenoxazinone synthase

1.3.2 Metal complexes as protein binding agents:

Serum albumins are the richest proteins found in biological systems. These proteins can be considered as a unique model for several biochemical and physiochemical reports [64]. These proteins have been playing a vital role in transporting a variety of exogenous and endogenous substances in blood having a restricted number of binding sites of very diverse specificity [65,66]. Bovine serum albumin (BSA) presents 76% structure homology with human serum albumin due to which they have been studied extensively [64,67]. On the other hand, HSA contains three domains (I, II and III) that present the protein a heart shaped molecule form [68] and BSA comprises of three homologous domains (I, II, and III) in which each domain, in turn, is the product of two sub-domains. Information regarding the effectiveness of drugs and binding characteristics can be detected from the fluorescence quenching studies of HSA and BSA-metal complexes. Binding interaction between serum albumin and nickel tetrazolato complexes are limited and requires more studies for simplification [69].

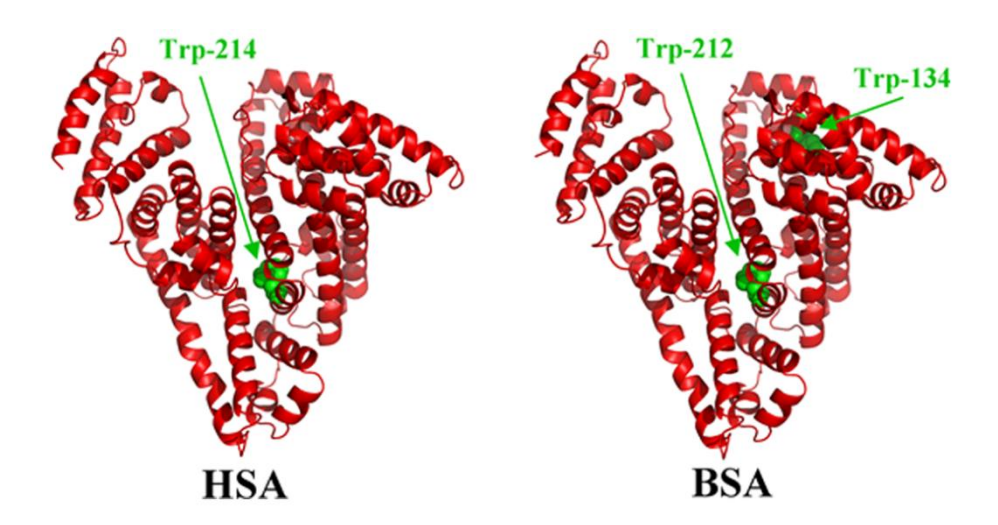


Figure 1.3: 3-D diagram of HSA and BSA

1.4 Organization of the thesis:

The aim of this project is to prepare different metal complexes from Schiff base ligand and tetrazoles and to find their probable applications in biochemistry.

Chapter 2: This chapter includes past work and project motivation.

Chapter 3: This chapter contains the materials, instrumentation, and experiments for the formation of transition metal complexes of tetrazoles and Schiff base ligand. Second part of this chapter includes the experimental techniques used to study phenoxazinone synthase like activity and BSA interactions.

Chapter 4: In this chapter, the results obtained have been discussed after synthesis and application study of the metal complexes are described.

Chapter 5: This chapter contains the conclusion of the project and also look forward to possible future scope and applications.

Chapter 2

Review of Past work and Project motivation

N, O-containing donor ligands specifically the salen type " N_2O_2 " donor symmetrical dicondensed Schiff base ligands have drawn attention of the synthetic chemists presumably because of their synthetic simplicity and ability to form metal complexes effortlessly with lots of probable applications [70-71]. Tetrazole ligand binds with metal ions very strongly. As they possess versatile binding sites, it has proven to be an interesting ligand in coordination chemistry [42]. Tetrazolato bridged polynuclear complexes containing Schiff base ligands are very rare, and their exploration has shown some unusual magnetic and catalytic properties [72].

2.1Biomimicking metalloenzyme

Kousik Ghosh *et al.* recently reported Co(III) complex *viz*. [Co (L- κ -N,N,O)(L- κ -N,O)(NCS)]·0.5H₂O.[73] The complex exhibited phenoxazinone synthase (PHS) and catechol oxidase mimicking activity. {HL = 2((2-morpholinoethylimino)methyl)-6-ethoxyphenol}

Mamoni Garai *et al.* reported tetranuclear zinc complex that has catalyzed the conversion of 2-aminophenol to phenoxazinine under the aerobic atmosphere [74].

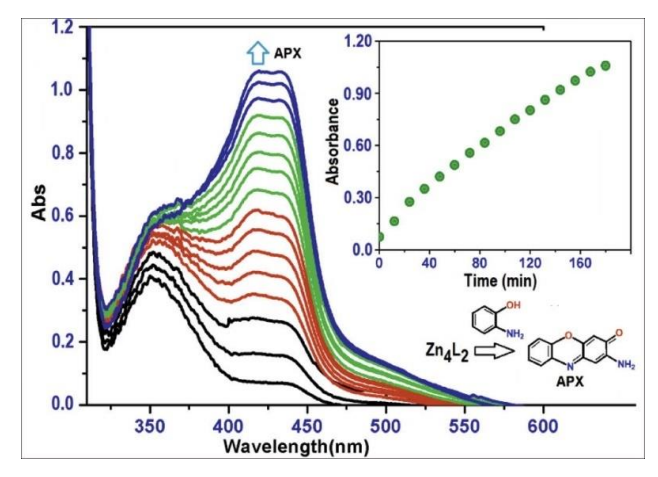


Figure 2.1: Spectra showing APX band at 434nm, recorded after every 11 min intervals.

Prithwish Mahapatra *et al.* proposed Cu complex of Schiff base which has been utilized to prepare two new complexes, $[(CuL)_2 Mn(N_3)(H_2O)](ClO_4)\cdot H_2O$; $[(CuL)_2Mn(NCS)_2]$ (where $H_2L = N-(2-hydroxyacetophenylidene)-N'-salicylidene-1,3-propanediamine).$

They found them catalytically active in mimicking phenoxazinone synthase (PHS) and catechol oxidase. Their complex shows the maximum catalytic activity in case of PHS among all of the reported complexes till date [75].

2.2 Biological Applications

The binding interaction of transition metal complexes with proteins (HSA and BSA) has been exhaustively examined due to their potent role as metallodrugs [76].

Novina Malviya *et al.* proposed the preparation of two nickel tetrazolato complex [NiL(5-phenyltetrazolato)]; [NiL $\{5-(4-pyridyl)-tetrazolato\}$] using 1,3-cycloaddition between [NiL(N₃)] [where HL = 3-(2-diethylamino-ethylimino)-1-phenyl-butan-1-one] and different organic nitriles. Both the above complexes show very promising interactions with HSA and BSA [31].

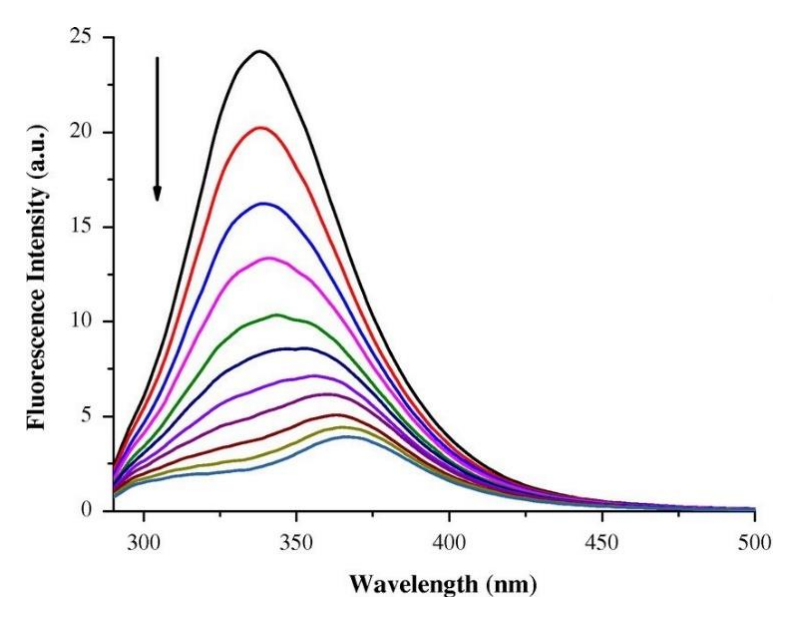


Figure 2.2: Fluorescence quenching by [NiL(5-phenyltetrazolato)] of BSA

2.3 Magnetic Properties

Exciting magnetic properties has been shown by the transition metal-Schiff base complexes.

Manideepa Saha *et al.* proposed the preparation of two trinuclear complexes, $[Ni_3L_2(5phenyltetrazolato)_4(DMF)_2]$ and $[Ni_3L_2\{5-(3-pyridyl)tetrazolato\}_4(DMF)_2]\cdot 2H_2O$ [77].

(where HL=*p*-chloro-2-{(2-(dimethylamino)ethylimino)methyl}phenol)

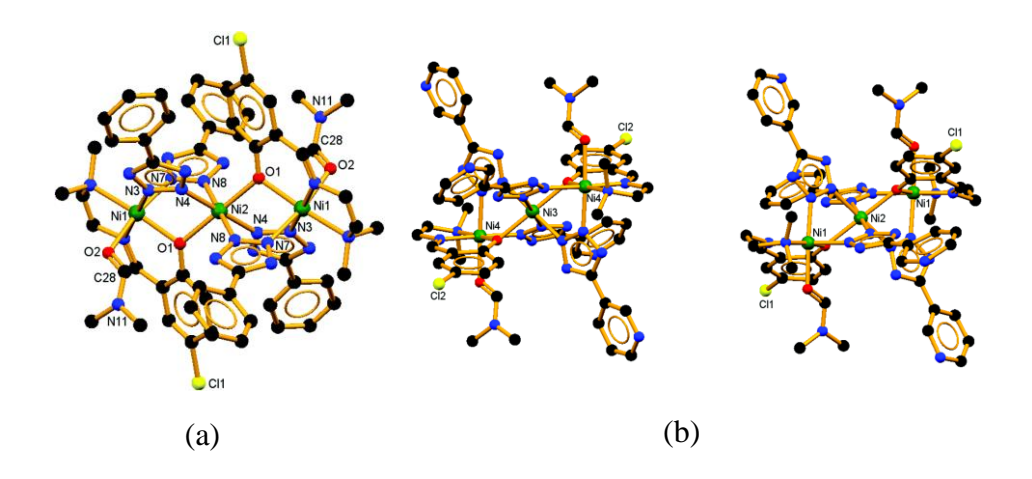


Figure 2.3: (a) Molecular structure of $[Ni_3L_2(5phenyltetrazolate)_4(DMF)_2]$ (b) Molecular structure of $[Ni_3L_2\{5-(3-pyridyl)tetrazolato\}_4(DMF)_2]\cdot 2H_2O$

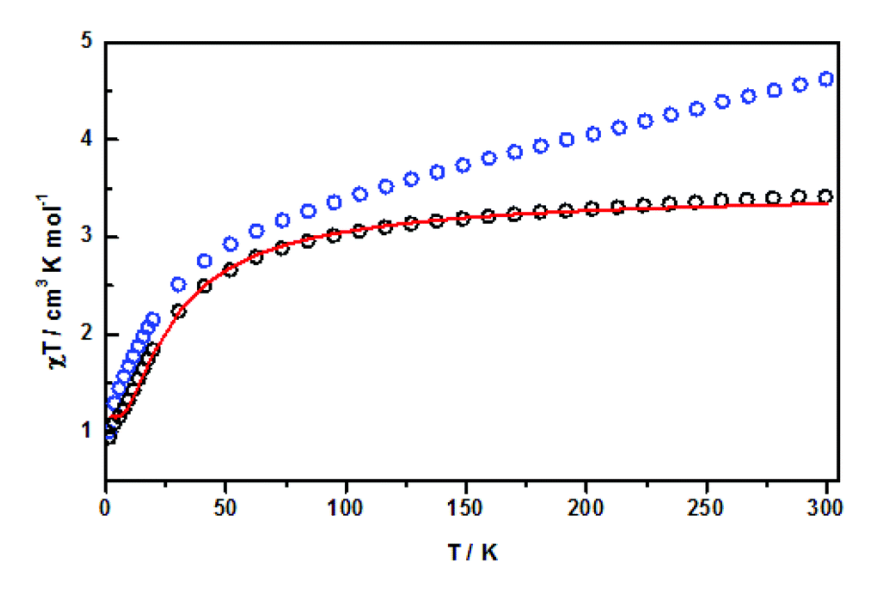


Figure 2.4: Molar susceptibility data were plotted for (a) and (b)

2.4 Gas adsorption

Metal tetrazole complexes exhibits good adsorption properties. Tien-Wen Tseng *et al.* has reported three tetrazole coordination compound polymers $[Mn(TzA)(H_2O)_2]_n$; (where $H_2TzA = 1H$ -tetrazole-5-acetic acid) $\{[Cd_5(MTz)_9]\cdot OH\}_n$; $[Cd_3(MTz)_3Cl_3]$ (where MTz = 5-methyltetrazolate) under hydrothermal conditions. At 77 K $[Cd_3(MTz)_3Cl_3]$ has shown significant absorption of hydrogen up to 80 cm³ g⁻¹ [78].

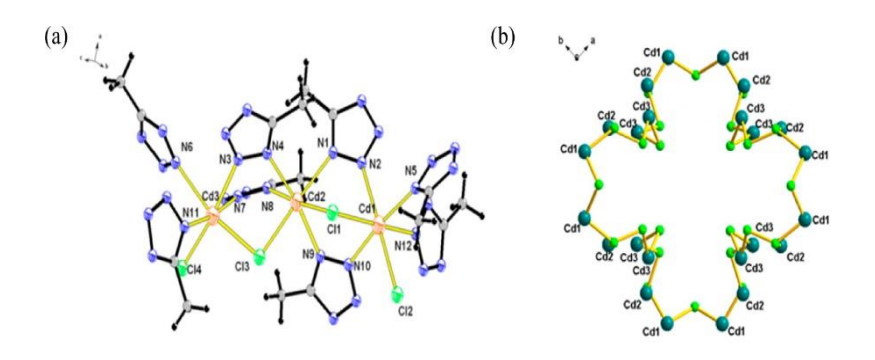


Figure 2.5: (a) ORTEP diagram of 3 showing three Cadmium centers (b) Displaying a 48-membered ring having Cd(II) cluster

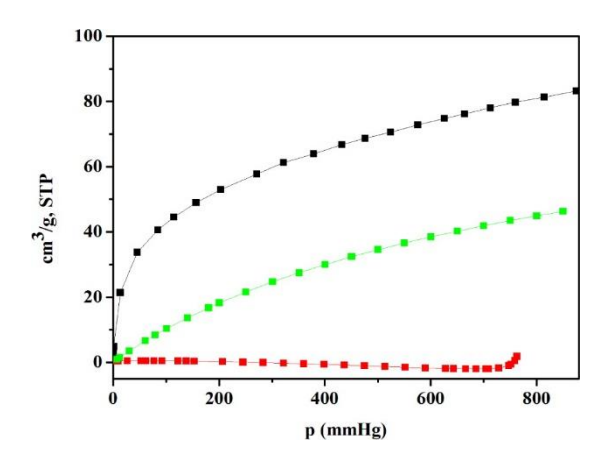


Figure 2.6: Gas adsorption isotherms (for CO₂ (green); for H₂ (black); for N₂ (red))

Experimental Section

3.1 Reagents and Chemicals

All the reagents and chemicals consumed were of analytical grade and utilized as received. These chemicals include *viz.* 1,3-propanediamine, salicylaldehyde, 4-chlorobenzonitrile, benzonitrile, sodium azide, ammonium chloride, triethylamine, and zinc nitrate were bought from Merck-India Chemical Company. nickel perchlorate hexahydrate was prepared in laboratory.

Caution! *Tetrazolate and azide compounds are known to be potentially explosive. Small amount of the compound should be prepared and handled with care.*

3.2 Methods and Instrumentation

Elemental analysis for carbon, hydrogen, nitrogen and sulfur was performed on a ThermoFlash 2000 elemental analyzer. IR spectra (4000 to 400 cm-1) were performed with FT-IR TENSOR 27 BRUKER instrument using KBr pellets. Electrospray ionization mass spectrometry (ESI-MS) was performed on Bruker-Daltonics, microTOF-Q II mass spectrometer. NMR spectra were recorded on ADVANCE III 400 Bruker Ascend BioSpin machine ambient temperature Spectrophotometric measurements were performed on a UV-Vis/NIR spectrophotometer (Model: Perkin-Elmer Lambda 750) and for emission, a Fluoromax-4p spectrofluorometer of Horiba JobinYvon (Model: FM-100) using a quartz cuvette with 1 cm path length.

3.3 X-ray Crystallography

Colorless cubic-shaped single crystals of complex 1, brown colored needle-shaped crystals of complex 2 and brown colored cubic-shaped single crystals of complex 3 was used for the X-ray crystallographic

analysis. Single crystal X-ray diffraction analysis of 1, 2 and 3 was done on CCD Agilent Technologies (Oxford Diffraction) SUPER NOVA diffractometer. Crystallographic data for the complexes 1, 2 and 3 were collected at 293 K using graphite-monochromated MoK α ($\lambda\alpha$ = 0.71073 Å) radiation. The CrysAlisPro CCD software was used to evaluate the strategy for the data collection. Standard 'phi-omega' scan techniques was employed to collect the data which was scaled and reduced using CrysAlis-ProRED software. SHELXS-97 was used as the direct method for solving the obtained structure of complex and it was refined by using full matrix least squares with SHELXS-97, refining on F². Locations of all the atoms of the structure were acquired using direct methods. The non-hydrogen atoms were refined anisotropically. The other hydrogen atoms were refined with isotropic temperature factors usually 1.2 Ueq of their parent atoms and were located in geometrically constrained positions [79].

3.4 Synthesis of Schiff base ligand and its metal complexes

3.4.1 Synthesis of Schiff base ligand (H_2L)

Schiff base ligand was synthesized according to a previously reported standard method [80]. A solution of 1,3-propanediamine (0.84 mL, 10 mmol) in 20 mL of methanol was added slowly to a 15 mL methanolic solution of salicylaldehyde (2.12 mL, 20 mmol). Then reaction mixture was refluxed for 4 h with stirring at 70 °C. After the evaporation of the solvent, the yellow colored crystalline solid product was formed with the addition of diethyl ether. The solid product obtained was dried and stored in a desiccator over anhydrous CaCl₂. Yield: 66.2%.

3.4.2 Synthesis of 5-phenyl-1H-tetrazole ligand

5-phenyl-1-*H*-tetrazole was prepared by standard procedure [81] by adding benzonitrile (1 mL, 9.70 mmol), sodium azide (0.94 g, 14.55 mmol) and NH₄Cl (0.51 g, 14.55 mmol) in 10 mL of DMF solvent and

refluxing it for 24 h at 130°C. The product was extracted with water after cooling to room temperature. Aqueous layer was acidified by adding 36% HCl dropwise to salt out the product. Yield: 72%.

3.4.3 Synthesis of 5-(4-chlorophenyl)-1-H-tetrazole ligand

5-(4-chlorophenyl)-1-*H*-tetrazole was prepared by standard procedure [81] by adding 4-chlorobenzonitrile (1.76 g, 9.70 mmol), sodium azide (0.94 g, 14.55 mmol) and NH₄Cl (0.51 g, 14.55 mmol) in 10 mL of DMF solvent and refluxing it for 24 h at 130 °C. The product was extracted with water after cooling to room temperature. Aqueous layer was acidified by adding 36% HCl dropwise to salt out the product. Yield: 76%.

3.4.4 Synthesis of $[Zn_3(L)_2(NO_3)_2]$

Solution of $\mathbf{H}_2\mathbf{L}$ (0.28 g, 1 mmol), triethylamine (550 μ L, 4 mmol) and zinc nitrate (0.28 g, 1.5 mmol) in 12 mL of methanol was packed in Teflon-lined stainless-steel vessel (25 mL) and it was kept in autoclave with temperature set at 110 °C for 72 h. After that it was allowed to cool at a rate of 5°C/ h⁻¹ to room temperature. Colorless cubic-shaped single crystals of complex **1** appropriate for X-ray diffraction were isolated and was washed with ethanol-water for further analysis. Yield: 84% (based on metal salt). Anal. Calculated (%): $C_{34}H_{32}N_6O_{10}Zn_3$ C, 46.36; H, 3.66; N, 9.54. Found (%): C, 46.40; H, 3.64; N, 9.60.

3.4.5 Synthesis of $[Ni_3(L)_2\{5-(4-chlorophenyl)-tetrazolato\}_2 (DMF)_2]$

Solution of $\mathbf{H_2L}$ (0.2 g, 0.708 mmol), triethylamine (1 mL), nickel perchlorate (0.27 g, 1.06 mmol), 5-(4-chlorophenyl)-1-*H*-tetrazole (0.13 g, 0.71 mmol) in methanol-DMF (1:1) mixture (12 mL) was packed in Teflon-lined stainless steel vessel (25 mL) and it was kept in autoclave with temperature set at 110 °C for 72 h. Later it was allowed to cool at a rate of 5°C/ h^{-1} to room temperature. Brown colored needle-shaped crystals of **2** appropriate for X-ray diffraction were isolated and was

washed with diethyl ether for further analysis. Yield: 15.1% (based on metal salt). Anal. Calculated (%): $C_{54}H_{54}Cl_2N_{14}Ni_3O_6$ C, 52.22; H, 4.38; N, 15.79. Found (%): C, 52.11; H, 4.39; N, 15.85.

3.4.6 Synthesis of $[Ni_3(L)_2\{5\text{-phenyltetrazolato}\}_2(DMF)_2]$

Solution of **H₂L** (0.2 g, 0.708 mmol), triethylamine (1 mL), nickel perchlorate (0.27 g, 1.06 mmol), 5-phenyl-1-H-tetrazole (0.1 g, 0.71 mmol) in methanol-DMF (1:1) mixture (12 mL) was packed in Teflonlined stainless steel vessel (25 mL) and it was kept in autoclave with temperature set at 110 °C for 72 h. Later it was allowed to cool at a rate of 5°C/ h⁻¹ to room temperature. Brown colored cubical-shaped single crystals of **2** appropriate for X-ray diffraction were isolated and was washed with diethyl ether for further analysis. Yield: 17.6% (based on metal salt). Anal. Calculated (%):C₅₄H₅₆N₁₄Ni₃O₆ C, 55.28; H, 4.81; N, 16.71. Found (%):C, 55.28; H, 4.89; N, 16.45.

3.5 BSA Binding study

The ability of nickel complexes (2,3) to bind with BSA protein was carried out by means of fluorescence spectroscopy by taking excitation at 295 nm and monitoring the emission at 340 nm using a Fluoromax spectrofluorometer with a cuvette of path length 1 cm. Buffered BSA protein stock solution in Tris-HCl (pH 7.4) was used. Solutions of complexes 2 and 3 (1mM) were made individually in Tris-HCl buffer and 5% DMSO. Fluorescence intensity of 2 mL stock solution of BSA was recorded as blank. Afterwards, titrations were done by successive additions of 5 μ L of the particular stock solution of complexes (up to 50 μ L). Further the Fluorescence data was examined using the Stern–Volmer equation and Scathard equation [31].

3.6 HSA binding study

The ability of nickel complexes (2,3) to bind with HSA was carried by

means of fluorescence spectroscopy by taking excitation at 295 nm and monitoring the emission at 340 nm using a Fluoromax spectrofluorometer with a cuvette of path length 1 cm. Buffered HSA protein stock solution in Tris-HCl (pH 7.4) was used. Solutions of complexes 2 and 3 (1mM) were made individually in Tris-HCl buffer and 5% DMSO. Fluorescence intensity of 2 mL stock solution of HSA was recorded as blank. Afterwards, titrations were done by successive additions of 5 μ L of the particular stock solution of complexes (up to 50 μ L). Further the Fluorescence data was examined using the Stern–Volmer equation and Scathard equation [31].

3.7 Catalytic oxidation of 2-AP to 2-aminophenoxazinone

To analyze the phenoxazinone synthase like mimicking activity (PHS), the reaction between 2-AP and molecular oxygen in the presence of trinuclear complex **1** was carried out. The ethanolic solution of 10^{-4} M of **1** was prepared and added to the 100 equivalents of ethanolic solution of 2-AP (10^{-2} M) at room temperature under aerobic atmosphere. Further, the absorbance was observed in the wavelength range of 300-800 nm at a fixed time interval of 10 minutes up to 90 minutes to observe the formation of the phenoxazinone band from 2-aminophenol oxidation [74]. Also, kinetic experiments were carried out during the course of catalysis using the trinuclear complex with 2-aminophenol in ethanol at 298 K in aerobic condition. The formation of 2-aminophenoxazinone from 2-aminophenol was observed using scan time at a fixed wavelength of 421 nm [82].

3.8 <u>Detection of hydrogen peroxide during the oxidation</u> reaction

Detection of H_2O_2 that is liberated during the course of catalytic oxidation can be found out by utilizing the modified iodometric method. For this purpose, the reaction mixtures were prepared as before. Quinone

imine is formed during the reaction which was extracted by adding equal volume of water by dichloromethane after 50 minutes of the reaction. Acidification of the aqueous layer was done by the dropwise addition of dilute H_2SO_4 and to stop the reaction and KI (1 mL, 10%) and ammonium molybdate (3 drops, 3%) were also added. The presence of H_2O_2 oxidized the Γ to iodine and iodide ions formed in excess results in the formation of triiodide ion.

$$H_2O_2 + 2\Gamma^- + 2H^+ \rightarrow 2H_2O + I_2$$

 $I_2 \text{ (aqueous)} + \Gamma^- \rightarrow I_3^-$

Reaction rate increased on consequent additions of the dilute sulfuric acid and condensation of the reaction was achieved immediately by adding ammonium molybdate. The convenient monitoring of triiodide ion was accomplished by observing the I_3^- band at $\lambda_{max} = 353$ nm using UV-Vis spectroscopy [83].

Chapter 4

Results and Discussion

4.1 Syntheses and Characterization

N₂O₂ symmetrical Schiff base ligand (H₂L) was synthesized according to the previously reported standard procedure [80] by mixing propanediamine (0.84 mL, 10 mmol) and 20 mmol of salicylaldehyde in 30 mL of methanol.

5-phenyl-1-*H*-tetrazole was synthesized according to the previously reported standard method [81] by refluxing the mixture of 9.70 mmol of benzonitrile, 14.55 mmol of sodium azide and 14.55 mmol of ammonium chloride in 10 mL of DMF. 5-(4-chlorophenyl)-1-*H*-tetrazole was prepared by refluxing the mixture of 9.70 mmol of 4-chlorobenzonitrile, 14.55 mmol of sodium azide and 14.55 mmol of ammonium chloride in 10 mL of DMF.

Trinuclear Zn(II) Schiff base complex was prepared by mixing of methanolic solution of zinc(II) nitrate to the methanolic solution of tetradentate N₂O₂ salen type symmetrical Schiff base in 3:2 mole ratio under the solvothermal condition of temperature 110 °C. The colorless crystals were obtained and structure elucidation of **1** was done through various analytical techniques including X-ray Diffraction analysis.

Upon reaction of ligand H₂L with Nickel perchlorate (2:3) in methanol-DMF mixture in the presence of triethylamine and 2 molar ratios of 5-(4-chlorophenyl)-1-*H*-tetrazole under solvothermal conditions, brown colored needle-like crystals were obtained. The structure elucidation of **2** was done through various analytical techniques, including X-ray Diffraction analysis.

Complex 3 was synthesized following the similar experimental procedures as done for 2. The structure elucidation of 3 was done through various analytical techniques, including X-ray Diffraction analysis.

ESI-MS spectrometry and ^{1}H and ^{13}C NMR spectroscopy have been performed to characterize ligands $H_{2}L$, 5-Phenyl-1-H-tetrazole and 5-(4-chlorophenyl)-1-H-tetrazole.

ESI-MS spectroscopy, elemental analyses, IR have been utilized to characterize all the complexes. Good quality crystals were obtained for 1,2 and 3 to characterize crystalographically.

Synthesis of Schiff Base ligand H₂L

Ligand H₂L

Scheme 4.1: Reaction Scheme for the synthesis of Schiff base ligand H₂L.

Synthesis of 5-substituted-1-*H*-tetrazole ligand

CN NaN₃/NH₄Cl DMF, 130 °C 24 h

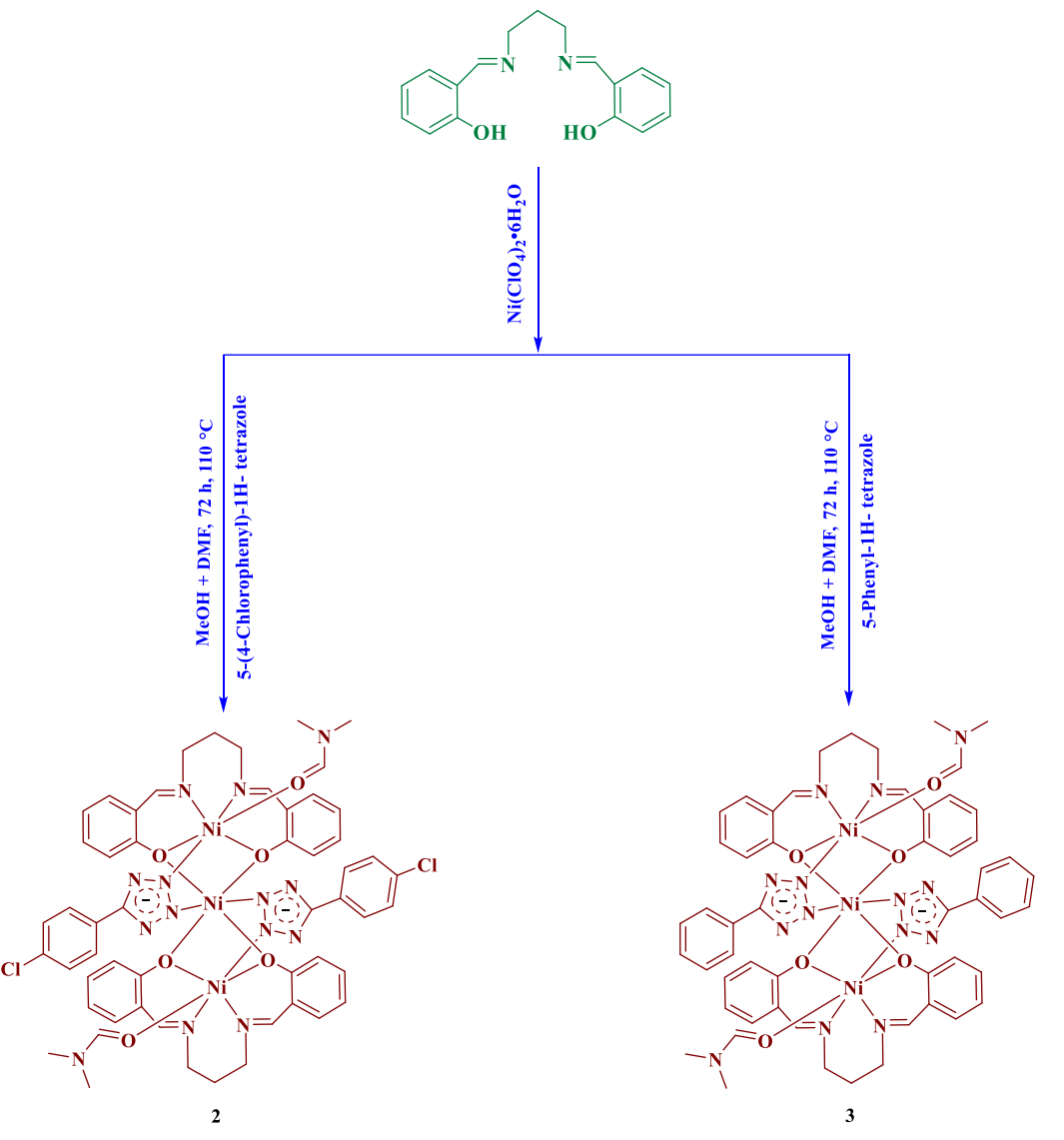
$$R = -H, -Cl$$

Scheme 4.2: Reaction Scheme for the synthesis of 5-substituted-1-*H*- tetrazole ligand

22

Synthesis of trinuclear zinc (II) complex from Schiff base ligand $H_2L \\$

Scheme 4.3: Scheme for the synthesis of $[Zn_3(L)_2(NO_3)_2]$ Synthesis of trinuclear Nickel complexes from Schiff base ligand H_2L and 5-substituted-1-*H*-tetrazole ligand as a bridging ligand



Scheme 4.4: Schematic route for the synthesis of nickel complexes from H₂L and 5-substituted-1-*H*-tetrazole ligand

4.1.1 NMR Spectra

The NMR data was found to be in good agreement for proposed structure of the ligands H_2L and 5-substituted-1-H- tetrazoles. (Figure 4.1-4.4)

For H₂L chemical shift value: ¹H NMR (400 MHz, CDCl₃): δ 13.43 (2 H, s, OH), 8.36 (2 H, s, -CH⁽⁷⁾), 7.3 (2 H, t, J = 8 Hz, Ar-H⁽³⁾), 7.24 (2 H, d, J = 8 Hz, Ar-H⁽¹⁾), 6.96 (2 H, d, J = 8 Hz, Ar-H⁽²⁾), 6.87 (2 H, t, J = 6 Hz, Ar-H⁽⁴⁾), 3.70 (4 H, t, J = 6 Hz, -NCH₂⁽⁶⁾), 2.11 (2 H, p, J = 6 Hz, -CH₂-⁽⁵⁾) ppm (Figure 4.4)

In 13 C NMR data of ligand H₂L, 8 peaks were observed. All the aromatic carbons were observed in between $\delta = 117.02$ to 132.32 ppm and phenolic carbon (attached to –OH group) was observed at $\delta = 165.50$ ppm.

In 1 H NMR spectra of 5-phenyl-1-*H*-tetrazole, all the five aromatic protons appear in between $\delta = 7.60$ to 8.04 ppm. 1 H NMR spectra of 5-(4-chlorophenyl)-1-*H*-tetrazole has all the four aromatic protons lie in between range of $\delta = 7.69$ to 8.05 ppm.

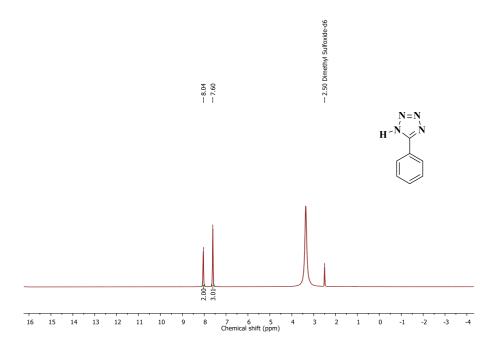


Figure 4.1: ¹H NMR data of 5-phenyl-1-*H*-tetrazole ligand

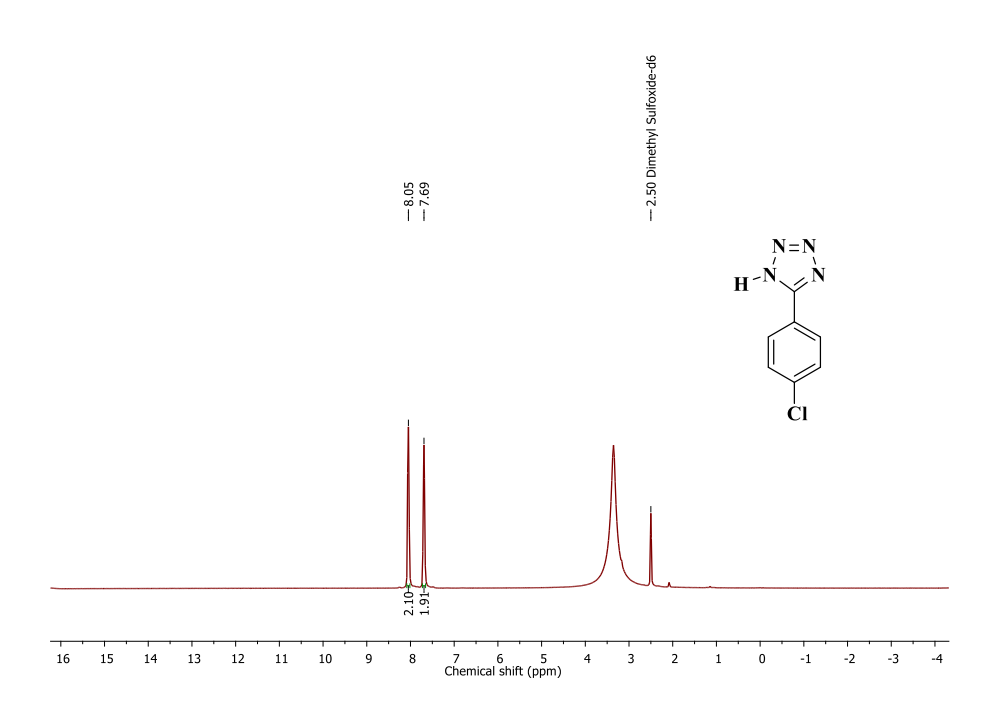


Figure 4.2: ¹H NMR data of 5-(4-chlorophenyl)-1-*H*-tetrazole ligand

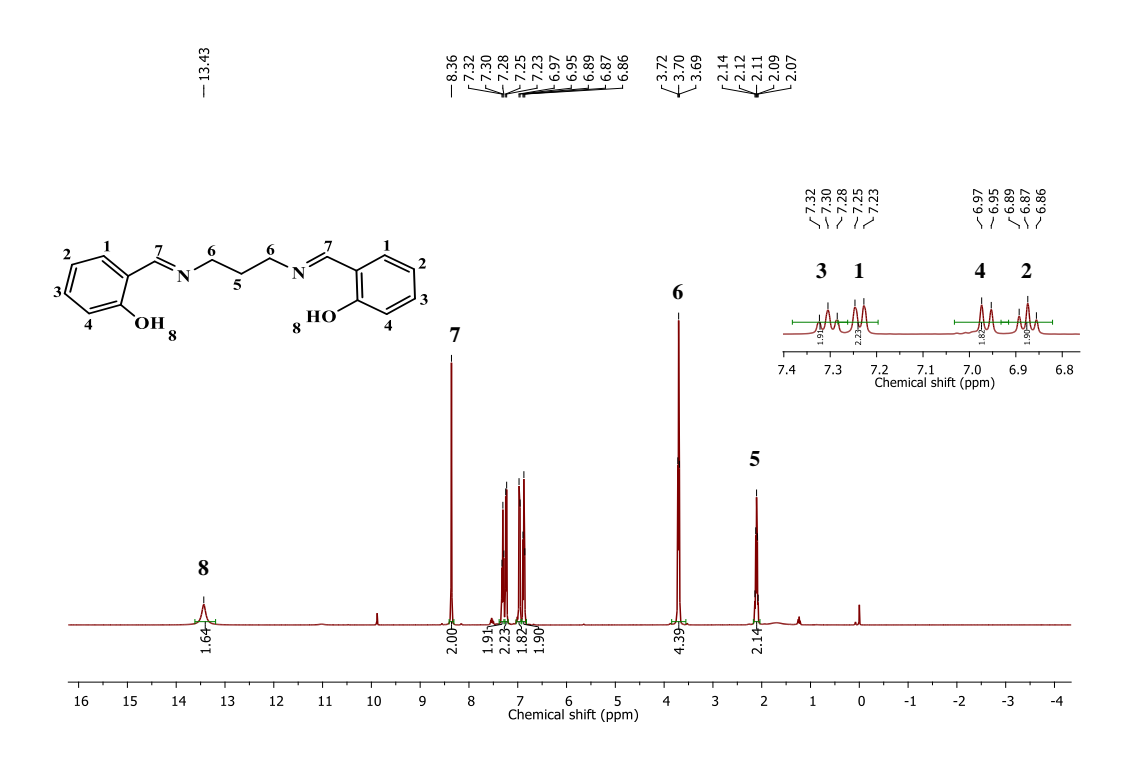


Figure 4.3: ¹H NMR data of Schiff base ligand H₂L

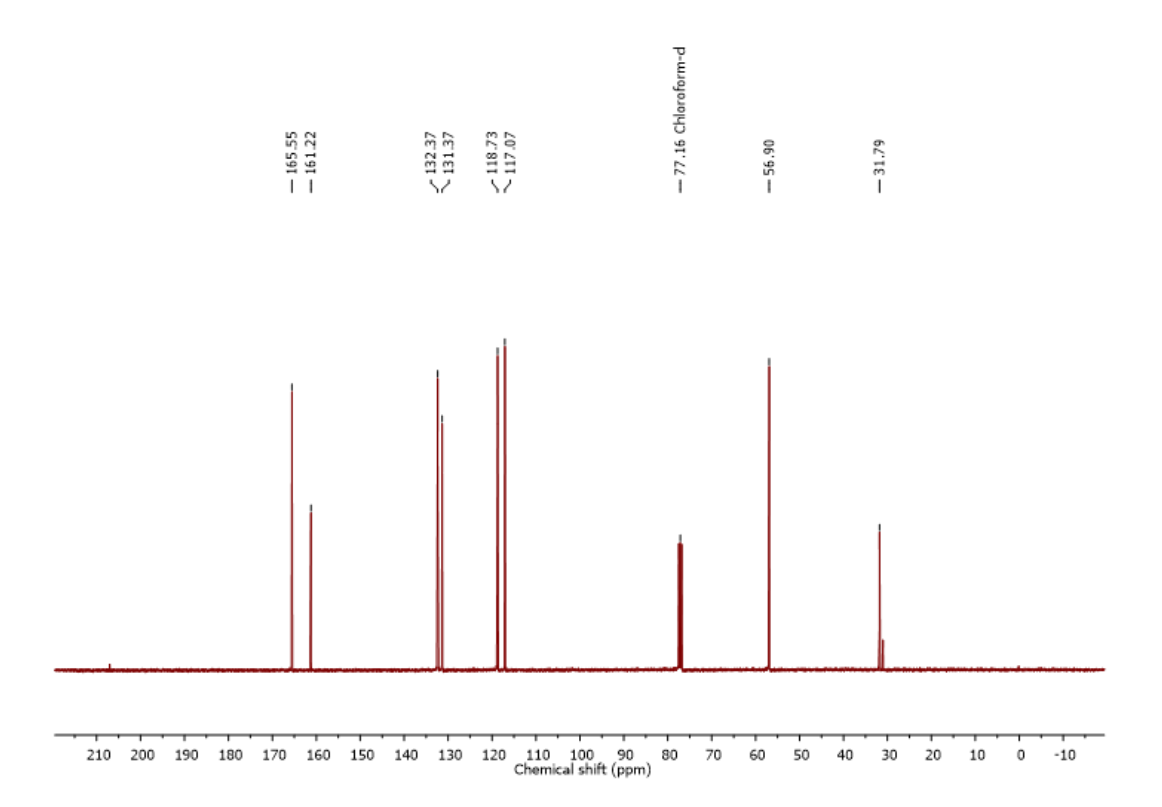


Figure 4.4: ¹³C NMR data of Schiff base ligand H₂L

4.1.2 Mass Spectra

The ESI-MS of Schiff base ligand (H_2L), 5-substituted-1-H- tetrazole and their complexes provide reliable confirmation for the preparation of the proposed compounds. HRMS of Schiff base ligand H_2L shows $[M+H]^+$ at m/z value at 283.14 and for 5-phenyl-1-H-tetrazole and 5-(4-chlorophenyl)-1-H-tetrazole ligand shows $[M-H]^-$ (molecular ion peak) m/z value at 145.07 and 179.03. However, the ESI-MS of the zinc complex 1 shows $[M+H]^+$ molecular ion peak at 881.1.

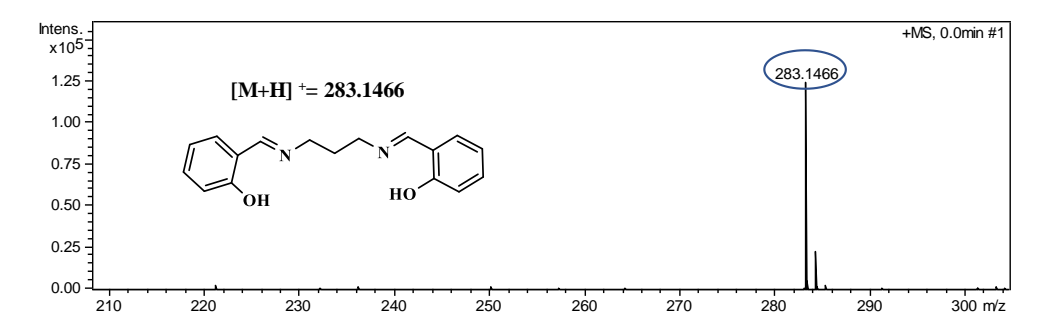


Figure 4.5: HRMS of Schiff base ligand H₂L

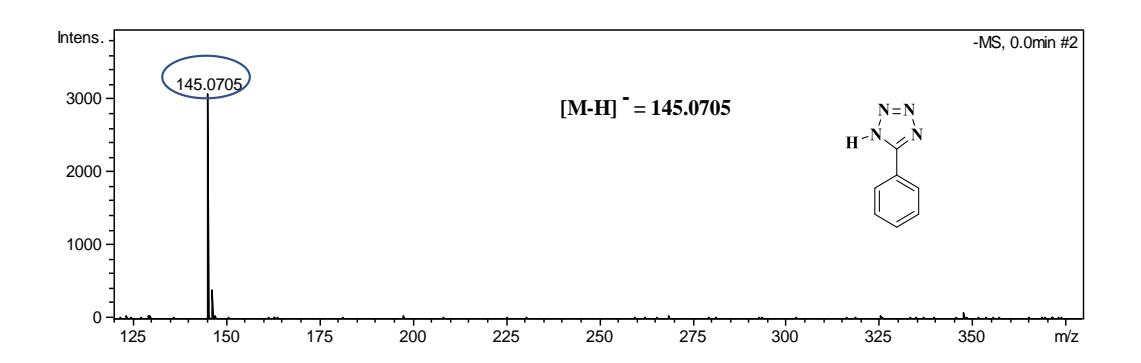


Figure 4.6: HRMS of 5-phenyl-1-*H*-tetrazole

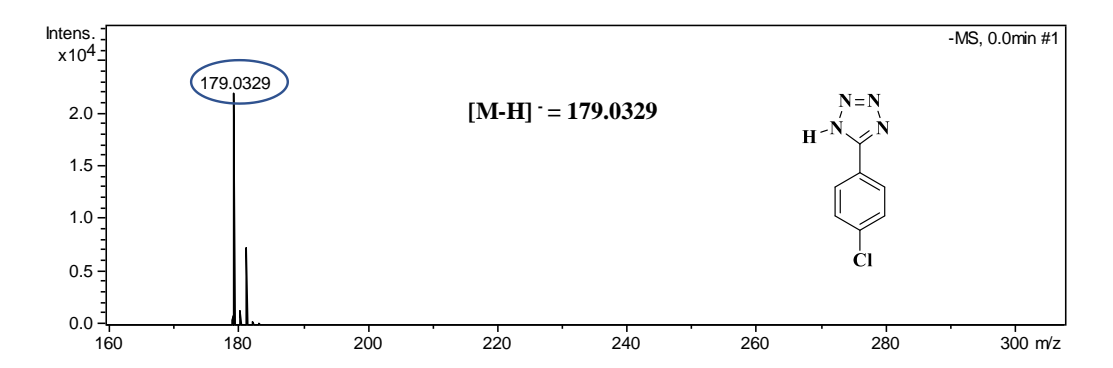


Figure 4.7: HRMS of 5-(4-chlorophenyl)-1-*H*-tetrazole.

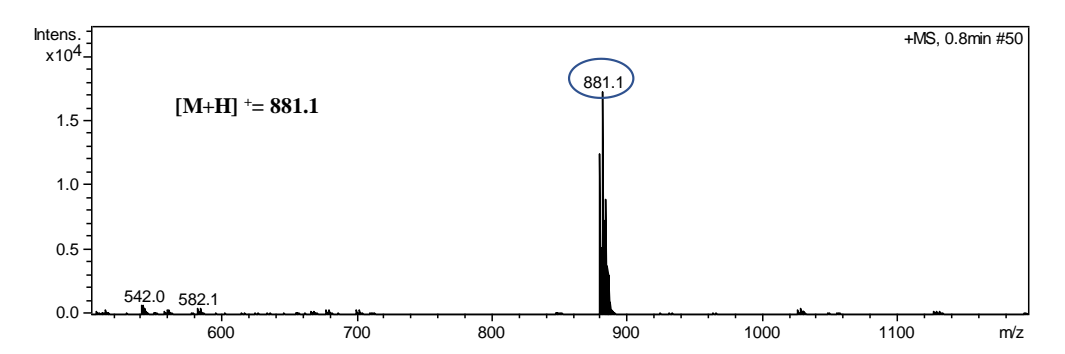


Figure 4.8: ESI-MS of $[Zn_3(L)_2(NO_3)_2]$

4.1.3 FT-IR spectra:

The IR data of the trinuclear zn(II) complex has a band around 1622 cm-1 which corresponds to $\bar{\upsilon}(\text{-C=N-})$ imine stretching mode (Figure 4.9). The IR data of the other three nickel tetrazolato complexes (2, 3) have a prominent band around 1565-1600, which corresponds to N-H bending mode of tetrazole moiety (Figure 4.10-4.11).

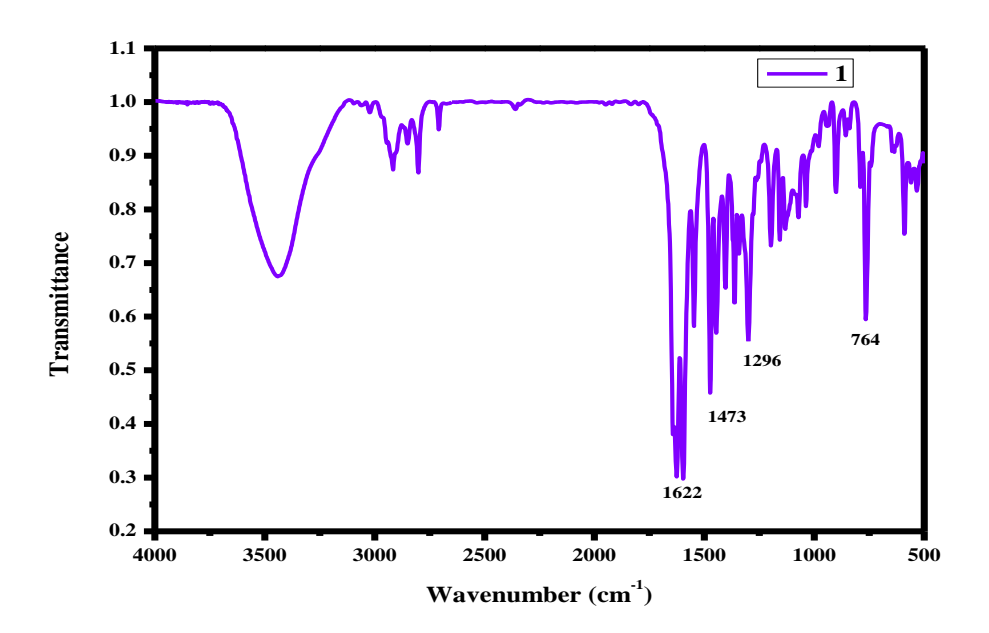


Figure 4.9: IR spectrum of 1

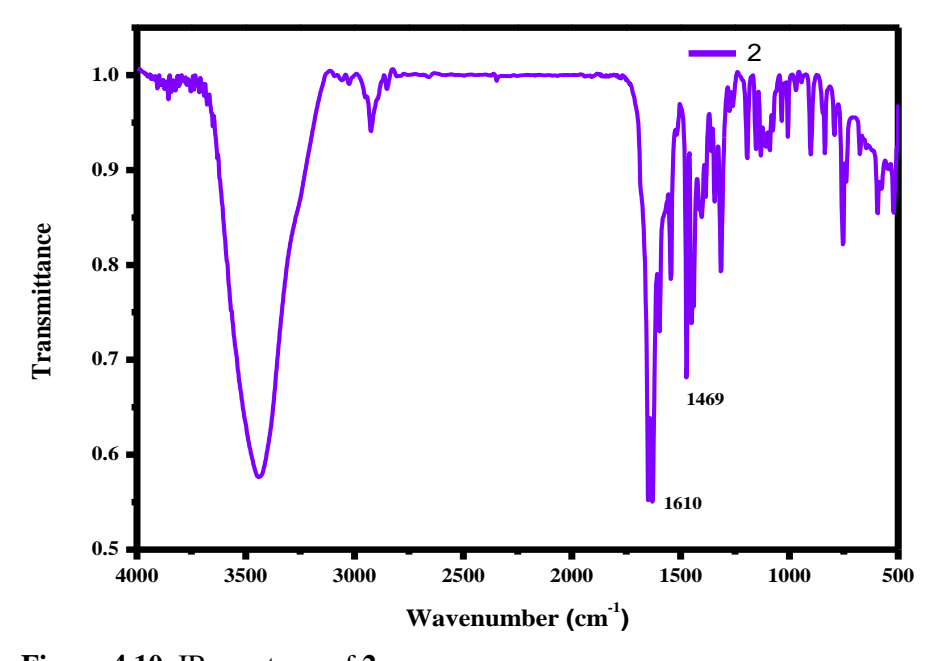


Figure 4.10: IR spectrum of 2

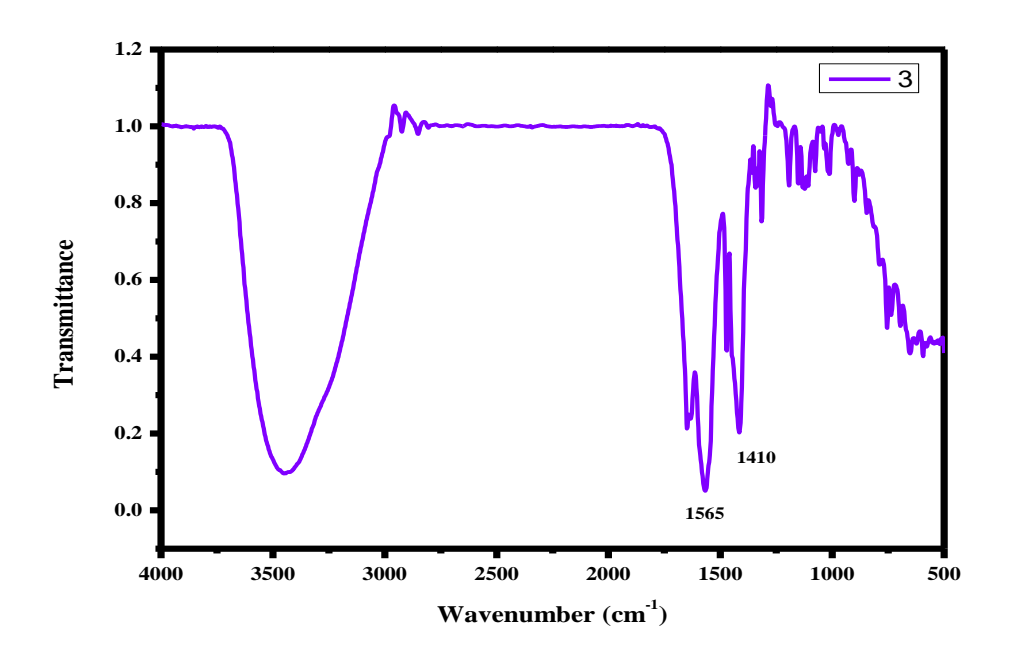


Figure 4.11: IR spectrum of 3

4.1.4 X- Ray Crystallography

Crystal structure description of [Zn₃(L)₂(NO₃)₂]

X-ray crystallography has been used to characterize the structure of Zn(II) complex. Figure 4.12 represents the molecular diagram of the complex. X-ray diffraction analysis shows that the complex has 3:2 metal to ligand stoichiometry. The space group has been found to be $P2_1/c$ and it crystallizes in the monoclinic system. The complex structure contains dinitro bridged trinuclear Zn(II) centres. The terminal Zn(II) ions are penta-coordinated while central Zn(II) ion has an octahedral geometry. The value of τ =0.3 suggests that the terminal Zn(II) centre of 1 is best described with a square pyramidal geometry. The selected angles between metal and coordination atoms and bond lengths were found to be quite similar as compared to earlier reports [84]. The crystallographic refinement parameters, bond lengths and bond angles are presented in Table 4.1-4.3.

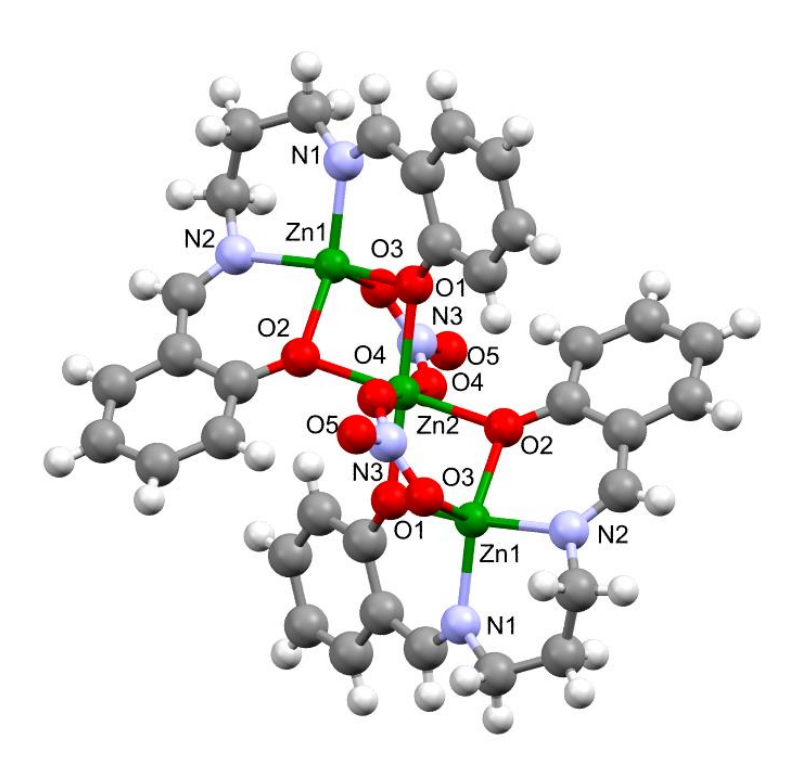


Figure 4.12: Crystal diagram of $[Zn_3(L)_2(NO_3)_2]$ showing the atom numbering scheme.

Table 4.1: Crystallographic refinement parameters for 1

Empirical Formula	C ₁₇ H ₁₆ N ₃ O ₅ Zn _{1.50}
Formula weight	440.38
Crystal system	Monoclinic
Space group	P 2 ₁ /c
a (Å)	9.2045(3)
b (Å)	11.6590(5)
c (Å)	16.6086(5)
α (°)	90
β (°)	99.900(3)
火 (°)	90
Volume, V (Å ³)	1755.82(11)
Wavelength, λ (Å)	0.71073
$\rho_{calcd} (mg m^{-3})$	1.666
Z	4
T(K)	293(2)
Absorption coefficient, μ (mm ⁻¹)	2.100
F (0 0 0)	896
Crystal size (mm³)	0.220 x 0.180 x 0.140

θ ranges (°)	2.947 to 29.129
Limiting indices, h/k/l	-11<=h<=12, -
	15<=k<=15, -22<=l<=21
Reflections collected / unique	23601 / 4373 [R(int) =
	0.0996]
Max. and min. transmission	1.00000 and 0.81678
Data/restraints/parameters	4373 / 1 / 237
Goodness-of-fit (GOF) on F^2	1.026
Final R indices $[I > 2\sigma(I)]$	R1 = 0.0626, wR2 =
	0.1347
R indices (all data)	R1 = 0.1326, $wR2 =$
	0.1706
Largest peak and hole (e Å ⁻³)	0.801 and -0.619
Completeness to theta = 25.242	99.9 %

Table 4.2: Selected bond lengths (\mathring{A}) for 1

2.008(5)
2.019(4)
2.047(5)
2.051(5)
2.054(4)
3.0245(6)
2.080(3)
2.080(3)
2.106(3)
2.106(3)
2.140(4)
2.141(4)
3.0245(6)

Table 4.3: Selected bond angles (°) for $\bf 1$

O(3)-Zn(1)-O(2)	105.71(17)	O(1)-Zn(1)-Zn(2)	43.32(9)
O(3)-Zn(1)-N(1)	108.12(19)	O(1)#1-Zn(2)-O(1)	180.0
O(2)-Zn(1)-N(1)	145.70(19)	O(1)#1-Zn(2)-O(2)#1	77.85(13)
O(3)-Zn(1)-N(2)	94.92(19)	O(1)-Zn(2)-O(2)#1	102.15(13)
O(2)-Zn(1)-N(2)	88.43(18)	O(1)#1-Zn(2)-O(2)	102.15(13)
N(1)-Zn(1)-N(2)	94.1(2)	O(1)-Zn(2)-O(2)	77.85(13)
O(3)-Zn(1)-O(1)	97.93(16)	O(2)#1-Zn(2)-O(2)	180.00(18)
O(2)-Zn(1)-O(1)	80.45(14)	O(1)#1-Zn(2)-O(4)	91.41(15)
N(1)-Zn(1)-O(1)	89.46(18)	O(1)-Zn(2)-O(4)	88.59(15)
N(2)-Zn(1)-O(1)	164.88(18)	O(2)#1-Zn(2)-O(4)	89.58(15)
O(3)-Zn(1)-Zn(2)	86.99(13)	O(2)-Zn(2)-O(4)	90.42(15)
O(2)-Zn(1)-Zn(2)	43.97(9)	O(1)#1-Zn(2)-O(4)#1	88.59(15)
N(1)-Zn(1)-Zn(2)	132.56(16)	O(1)-Zn(2)-O(4)#1	91.41(15)
N(2)-Zn(1)-Zn(2)	130.08(15)	O(2)#1-Zn(2)-O(4)#1	90.42(15)
O(2)-Zn(2)-O(4)#1	89.58(15)	Zn(1)#1-Zn(2)-Zn(1)	180.0
O(4)-Zn(2)-O(4)#1	180.0	C(1)-O(1)-Zn(1)	128.2(3)
O(1)#1-Zn(2)-Zn(1)#1	42.63(10)	C(1)-O(1)-Zn(2)	131.7(4)
O(1)-Zn(2)-Zn(1)#1	137.37(10)	Zn(1)-O(1)-Zn(2)	94.05(14)
O(2)#1-Zn(2)-Zn(1)#1	41.73(9)	C(17)-O(2)-Zn(1)	129.4(3)
O(2)-Zn(2)-Zn(1)#1	138.27(10)	C(17)-O(2)-Zn(2)	136.3(3)
O(4)-Zn(2)-Zn(1)#1	108.34(11)	Zn(1)-O(2)-Zn(2)	94.30(14)
O(4)#1-Zn(2)-Zn(1)#1	71.66(11)	N(3)-O(3)-Zn(1)	119.8(5)
O(1)#1-Zn(2)-Zn(1)	137.37(10)	N(3)-O(4)-Zn(2)	134.2(5)
O(1)-Zn(2)-Zn(1)	42.63(10)	C(7)-N(1)-Zn(1)	122.9(4)
O(2)#1-Zn(2)-Zn(1)	138.27(9)	C(8)-N(1)-Zn(1)	118.9(5)
O(2)-Zn(2)-Zn(1)	41.73(10)	C(11)-N(2)-Zn(1)	126.6(4)
O(4)-Zn(2)-Zn(1)	71.66(11)	C(10)-N(2)-Zn(1)	115.0(4)
O(4)#1-Zn(2)-Zn(1)	108.34(11)	C(7)-N(1)-C(8)	118.2(5)

Crystal structure description of $[Ni_3(L)_2\{5-(4-chlorophenyl)-tetrazolato\}_2(DMF)_2]$

Complex 2 is trinuclear with the triclinic crystal system and space group P-1. Figure 4.13 represents molecular structure of the complex. The molecular unit comprises of three Ni(II) ions with bridging 4-chlorophenyl tetrazolato ligands, symmetrical tetradentate Schiff base ligands. Each metal center is octahedrally coordinated. All are coordinated to the metal center through oxygen atom and nitrogen atom resulting in the expected octahedral geometry. The selected angles between metal and coordination atoms and bond lengths are found to be quite similar as reported previously [77]. The crystal refinement details, bond lengths and bond angles are presented in Table 4.4-4.6.

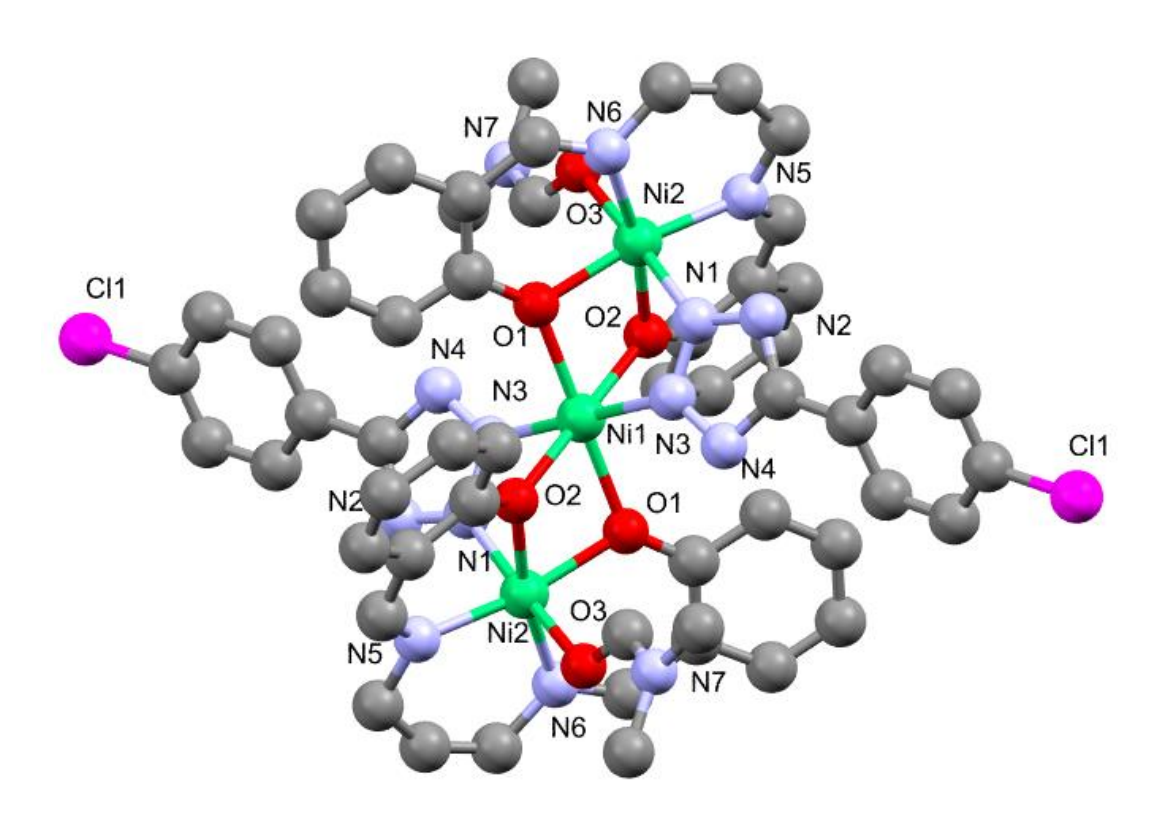


Figure 4.13: Crystal structure of $[Ni_3(L)_2\{5-(4-chlorophenyl)-tetrazolato\}_2(DMF)_2]$ showing the atom numbering. Hydrogen atoms are not shown for clarity.

 Table 4.4: Crystallographic refinement details for 2

Empirical Formula	C ₅₄ H ₅₄ Cl ₂ N ₁₄ Ni ₃ O ₆
Formula weight	1244.15
Crystal system	Triclinic
Space group	P-1
a (Å)	11.6693(10)
b (Å)	12.8746(9)
c (Å)	20.1742(15)
α (°)	74.488(2)
β (°)	86.101(3)
γ(°)	86.636(3)
Volume, $V(\mathring{A}^3)$	2911.2(4)
Wavelength, λ (Å)	0.71073
$\rho_{calcd} (mg m^{-3})$	1.419
Z	2
T(K)	273
Absorption coefficient, μ (mm ⁻¹)	1.112
F (0 0 0)	1288.0
θ max (°)	26.022
Limiting indices, h/k/l	14,15,24
Reflections, R	0.0543 (8577)
Packing coefficient	0.630297
Data completeness	0.992

Table 4.5: Selected bond lengths (\mathring{A}) for 2

Ni(1)-Ni(2)	3.0448	Ni(2)-O(3)	2.145(4)
Ni(1)-O(2)	2.064	Ni(2)-N(1)	2.112(4)
Ni(1)-O(1)	2.093	Ni(2)-O(1)	2.013(3)
Ni(1)-N(3)	2.088	Ni(2)-N(5)	2.014(4)
Ni(2)-O(2)	2.011(2)	Ni(2)-N(6)	2.016(3)

Table 4.6: Selected bond angles (°) for **2**

Ni(2)-Ni(1)-O(2)	40.99	O(1)-Ni(1)-N(3)	95.4
Ni(2)-N(1)-O(1)	41.13	N(3)-Ni(1)-N(3)	180.0
Ni(2)-Ni(1)-N(3)	65.5	Ni(1)-Ni(2)-O(2)	42.32
Ni(2)-Ni(1)-Ni(2)	180.0	Ni(1)-Ni(2)-O(3)	110.2
Ni(2)-Ni(1)-O(2)	139.01	Ni(1)-Ni(2)-N(1)	65.9
Ni(2)-Ni(1)-O(1)	138.87	N(1)-Ni(2)-O(1)	85.0(1)
Ni(2)-N(1)-N(3)	114.5	N(1)-Ni(2)-N(5)	92.0(2)
O(2)-Ni(1)-O(1)	76.1	N(1)-Ni(2)-N(6)	98.9(1)
O(2)-Ni(1)-N(3)	83.2	O(1)-Ni(2)-N(5)	169.7(1)
O(2)-Ni(1)-O(2)	180.0	O(1)-Ni(2)-N(6)	91.6(1)
O(2)-Ni(1)-O(1)	103.9	N(5)-Ni(2)-N(6)	98.6(2)
O(2)-Ni(1)-N(3)	96.8	Ni(1)-O(2)-Ni(2)	96.7
O(1)-Ni(1)-N(3)	84.6	Ni(1)-O(2)-C(8)	137.4
O(1)-Ni(1)-O(1)	180.0	Ni(2)-O(2)-C(8)	125.8(2)
Ni(1)-Ni(2)-O(1)	43.16	Ni(2)-O(3)-C(25)	121.3(4)
Ni(1)-Ni(2)-N(5)	126.8	Ni(2)-N(1)-N(2)	134.7(3)
Ni(1)-Ni(2)-N(6)	131.0	Ni(2)-N(1)-N(3)	112.8(3)
O(2)-Ni(2)-O(3)	90.3(1)	Ni(1)-O(1)-Ni(2)	95.7
O(2)-Ni(2)-N(1)	85.3(1)	Ni(1)-O(1)-C(24)	137.6
O(2)-Ni(2)-O(1)	79.1(1)	Ni(2)-O(1)-C(24)	126.7(3)
O(2)-Ni(2)-N(5)	90.9(1)	Ni(2)-N(5)-C(14)	123.4(4)
O(2)-Ni(2)-N(6)	169.4(1)	Ni(2)-N(5)-C(15)	119.8(4)
O(3)-Ni(2)-N(1)	175.5(1)	Ni(2)-N(6)-C(18)	121.7(3)
O(3)-Ni(2)-O(1)	93.6(1)	Ni(2)-N(6)-C(17)	119.9(3)
O(3)-Ni(2)-N(5)	88.6(2)	Ni(1)-N(3)-N(1)	115.7
O(3)-Ni(2)-N(6)	85.4(1)	Ni(1)-N(3)-N(4)	132.9

Crystal structure description of

$[Ni_3(L)_2{5-phenyltetrazolato}_2(DMF)_2]$

Complex 3 has been found to be trinuclear in nature with the triclinic crystal system and space group P-1. Figure 4.14 represents molecular structure of the complex. The molecular unit comprises of three Ni(II) ions with bridging phenyl tetrazolato ligands, symmetrical tetradentate Schiff base ligands. Each metal center is hexa-coordinated. All are coordinated to the metal center through oxygen atom and nitrogen-atom resulting in distorted octahedral geometry. The selected angles between metal and coordination atoms and bond lengths are found to be quite similar as reported previously [77]. Crystal refinement details, bond lengths and bond angles are presented in Table 4.7-4.9.

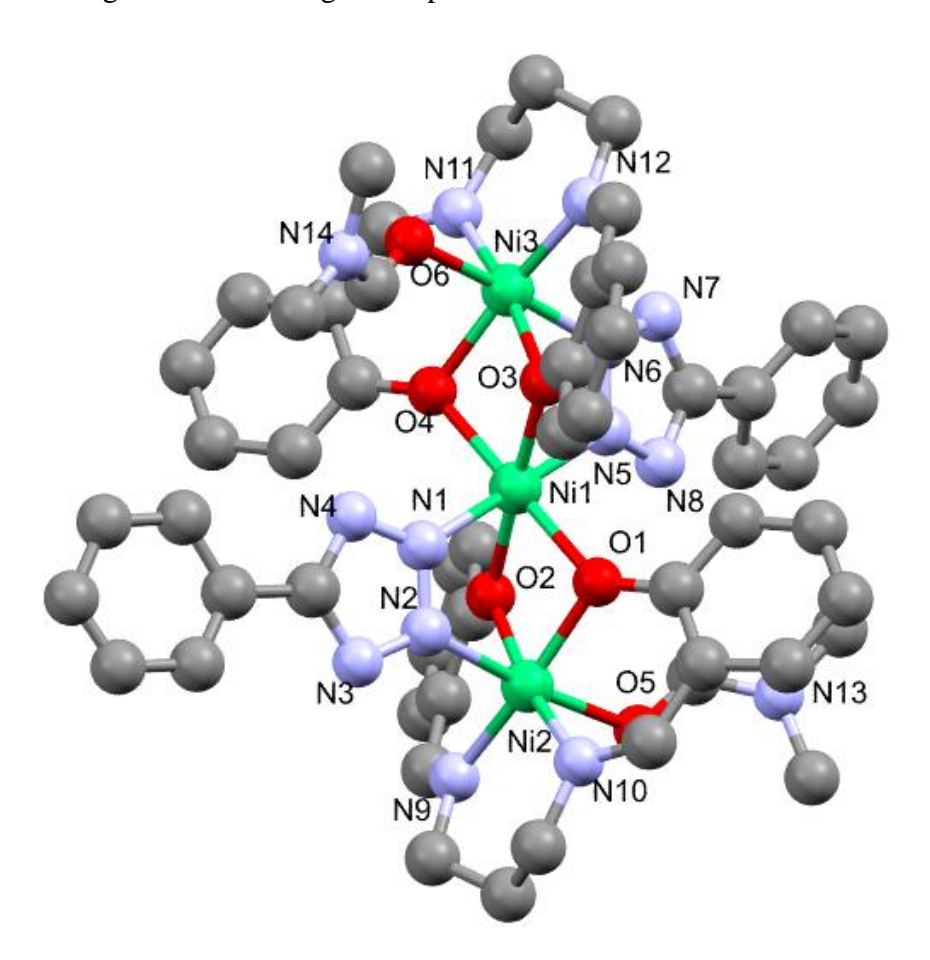


Figure 4.14: Crystal structure of $[Ni_3(L)_2\{5\text{-phenyltetrazolato}\}_2(DMF)_2]$ showing the atom numbering. Hydrogen atoms are not shown for clarity.

 Table 4.7: Crystallographic refinement details for 3

Empirical Formula	C ₅₄ H ₅₆ N ₁₄ Ni ₃ O ₆
Formula weight	1173.20
Crystal system	Triclinic
Space group	P-1
a (Å)	10.5170(3)
b (Å)	14.5886(5)
c (Å)	18.4385(6)
α (°)	85.596(1)
β(°)	76.811(1)
γ (°)	84.911(1)
Volume, $V(\mathring{A}^3)$	2738.84
Wavelength, λ (Å)	0.71073
$\rho_{calcd} (mg m^{-3})$	1.423
Z	2
T(K)	283-303
Absorption coefficient, μ (mm ⁻¹)	1.083
F (0 0 0)	1220.0
θ max (°)	26.022
Limiting indices, h/k/l	14,15,24
Packing coefficient	0.642221

Table 4.8: Selected bond lengths (Å) for **3**

Ni(2)-Ni(1)	3.0333(6)	Ni(2)-N(9)	2.003(3)
Ni(2)-O(5)	2.162(3)	Ni(2)-N(2)	2.101(3)
Ni(1)-O(1)	2.073(2)	Ni(1)-Ni(3)	3.0260(6)
Ni(2)-O(1)	2.018(2)	Ni(1)-O(2)	2.073(2)
Ni(2)-O(2)	2.017(2)	Ni(2)-N(10)	2.017(3)
Ni(1)-O(3)	2.053(2)	Ni(1)-N(5)	2.088(3)
Ni(1)-O(4)	2.091(2)	Ni(1)-N(1)	2.088(3)
Ni(3)-O(6)	2.159(3)	Ni(3)-N(6)	2.081(3)
Ni(3)-O(3)	2.017(2)	Ni(3)-N(12)	2.009(3)
Ni(3)-O(4)	2.016(2)	Ni(3)-N(11)	2.014(3)

Table 4.9: Selected bond angles (°) for $\bf 3$

Ni(1)-Ni(2)-O(5)	108.89(7)	Ni(2)-Ni(1)-N(5)	114.29(8)
Ni(1)-Ni(2)-O(2)	42.86(6)	Ni(2)-Ni(1)-N(1)	65.55(8)
Ni(1)-Ni(2)-O(1)	42.84(6)	Ni(3)-Ni(1)-O(2)	139.17(6)
Ni(1)-Ni(2)-N(10)	129.30(9)	Ni(3)-Ni(1)-O(1)	137.43(6)
Ni(1)-Ni(2)-N(9)	129.60(9)	Ni(3)-Ni(1)-O(3)	41.52(6)
Ni(1)-Ni(2)-N(2)	65.98(8)	Ni(3)-Ni(1)-O(4)	41.58(6)
O(5)-Ni(2)-O(2)	93.5(1)	Ni(3)-Ni(1)-N(5)	64.96(8)
O(5)-Ni(2)-O(1)	90.0(1)	Ni(3)-Ni(1)-N(1)	115.23(8)
O(5)-Ni(2)-N(10)	84.8(1)	O(2)-Ni(1)-O(1)	77.64(9)
O(5)-Ni(2)-N(9)	88.7(1)	O(2)-Ni(1)-O(3)	178.17(9)
O(5)-Ni(2)-N(2)	174.4(1)	O(2)-Ni(1)-O(4)	104.03(9)
O(2)-Ni(2)-O(1)	80.19(9)	O(2)-Ni(1)-N(5)	95.4(1)
O(2)-Ni(2)-N(10)	170.7(1)	O(2)-Ni(1)-N(1)	83.3(1)
O(2)-Ni(2)-N(9)	90.9(1)	O(1)-Ni(1)-O(3)	101.02(9)
O(2)-Ni(2)-N(2)	84.0(1)	O(1)-Ni(1)-O(4)	177.97(9)
O(1)-Ni(2)-N(10)	90.7(1)	O(1)-Ni(1)-N(5)	97.8(1)
O(1)-Ni(2)-N(9)	170.9(1)	O(1)-Ni(1)-N(1)	83.3(1)
O(1)-Ni(2)-N(2)	84.6(1)	O(3)-Ni(1)-O(4)	77.34(9)
N(10)-Ni(2)-N(9)	98.2(1)	O(3)-Ni(1)-N(5)	83.5(1)
N(10)-Ni(2)-N(2)	96.8(1)	O(3)-Ni(1)-N(1)	97.8(1)
N(9)-Ni(2)-N(2)	96.4(1)	O(4)-Ni(1)-N(1)	95.7(1)
Ni(3)-Ni(2)-Ni(3)	178.80(2)	N(5)-Ni(1)-N(1)	178.1(1)
Ni(2)-Ni(1)-O(2)	41.43(6)	Ni(1)-Ni(3)-O(6)	109.90(8)
Ni(2)-Ni(1)-O(1)	41.46(6)	Ni(1)-Ni(3)-O(3)	42.43(6)
Ni(2)-Ni(1)-O(3)	137.84(6)	Ni(1)-Ni(3)-N(6)	66.49(8)
Ni(2)-Ni(1)-O(4)	139.55(7)	Ni(1)-Ni(3)-N(12)	128.42(9)
Ni(1)-Ni(2)-O(5)	108.89(7)	Ni(2)-Ni(1)-N(5)	114.29(8)
Ni(1)-Ni(2)-O(2)	42.86(6)	Ni(2)-Ni(1)-N(1)	65.55(8)
O(6)-Ni(3)-N(6)	175.8(1)	O(6)-Ni(3)-N(11)	88.9(1)
O(6)-Ni(3)-N(12)	85.2(1)	O(6)-Ni(3)-O(4)	93.0(1)
O(12)-Ni(3)-N(4)	170.3(1)	O(3)-Ni(3)-N(11)	170.9(1)
	1	ı	

4.2 <u>Phenoxazinone synthase mimicking activity of the</u> trinuclear Zn(II) complex

Taking 2-AP as the standard substrate for the oxidation using the trinuclear Zn(II) complex under aerobic conditions and at 298 K in ethanol as solvent, spectro photochemical studies were performed. In the experiment, ethanolic solution of Zn(II) complex (10⁻⁴ M) was added to the ethanolic solution of 2-aminophenol (10⁻² M). UV-Vis spectrophotometer was utilized for the purpose of recording spectrophotometric scans for a duration of 90 mins at a time interval of 60 seconds. Literature reveals that 2-aminophenol shows a single peak at 267 nm [85]. Disappearance of this characteristic peak has been observed with time, with the formation of a new band at 421 nm during the course of oxidation reaction. This new band indicates the formation of an oxidized species in the solution [83,85]. Blank experiments were also done in the absence of the catalyst. Yield of phenoxazinone was very less due to autooxidation; thus, it was neglected in this case. The catalytic ability of Zn(II) compound has been further investigated using the kinetic studies. The rise in the absorbance peak corresponding to the phenoxazine-3-one at 421 nm was examined as a function of time at 298 K. Further, Michaelis-Menten approach was used to analyze the kinetics. V_{max} value has been divided with the concentration of complex 1 to obtain the value of the turnover number $(K_{cat} \text{ or TON})$. As summarized in Table 4.10 the values are, V_{max} (Ms⁻¹) = 1.22 × 10⁻⁴; K_m (M)= 0.00104 (Figure 4.16) and TON or $K_{cat}(h^{-1}) = 4.40 \times 10^3$. The value of TON of 1 is found to be higher than the previously reported tetranuclear zinc complex [74] and other metal complexes mimicking phenoxazinone synthase [86-88]. Catalytic efficiency (K_{cat}/K_m) of the complex was found quite high which is equal to 4.24×10^6 and suggestive of a very good catalytic efficacy for mimicking oxidation.

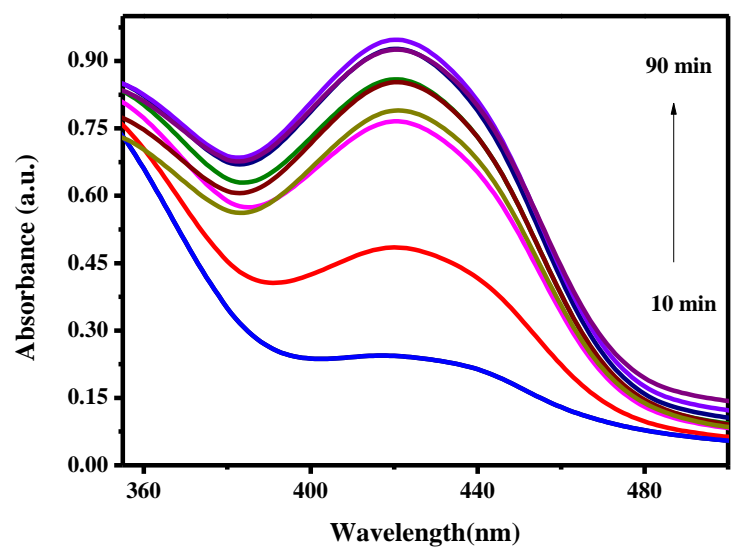


Figure 4.15: Spectra showing the growth of phenoxazinone species at 421 nm

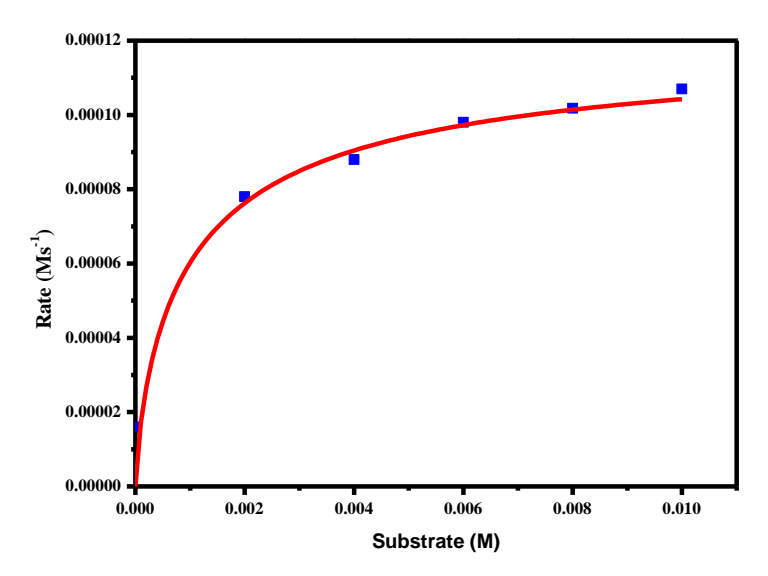


Figure 4.16: Michaelis-Menten kinetics plot between the rate of oxidation of 2-AP vs. concentration of 2-AP substrate in EtOH medium

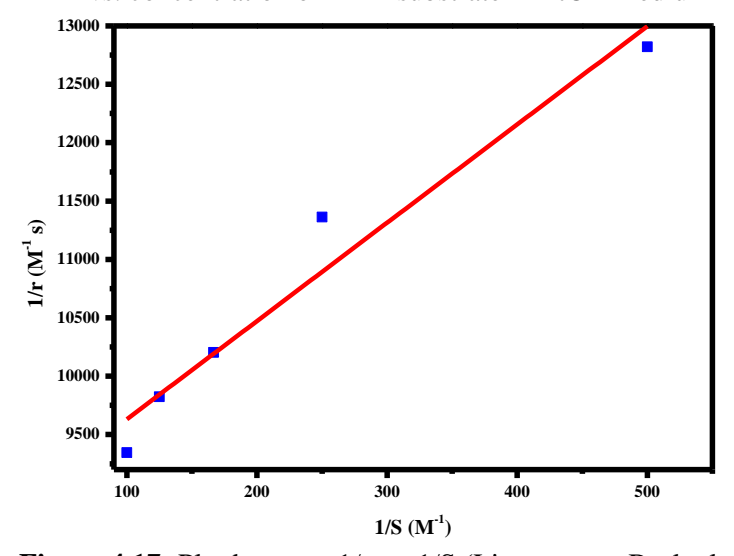


Figure 4.17: Plot between 1/r vs. 1/S (Lineweaver- Burk plot)

Table 4.10: Summary of kinetic parameters of phenoxazinone synthase (PHS) mimicking the activity of catalyst **1**

Catalyst	V _{max} (Ms ⁻¹)	Std. Error	K _m (M)	K _{cat} (h ⁻¹)
1	1.22×10^{-4}	9.86 × 10 ⁻⁵	1.04×10^{-3}	4.40×10^3

Mechanistic insight for catalytic oxidation of 2-AP

It is very unusual that similar functional activities of Cu(II) based metalloenzyme (PHS) is exhibited by Zn(II) Schiff base complex .To get a mechanistic insight of phenoxazinone synthase like activity shown by trinuclear Zn(II) complex, ESI-mass spectrometry has been performed in order to investigate the probable catalyst-substrate intermediate formation during catalytic oxidation. Positive mode ESI-MS spectrum (Figure 4.18) has been performed for ethanolic solution of 1 and 2-aminophenol (1:100) and was taken after every 10 min time intervals. Extensive fragmentation was observed in the obtained mass spectra for complex, substrate and catalyst-substrate intermediate. The spectra exhibit peak at 213, which corresponds to the phenoxazinoneproton aggregate [APX+H⁺] +. It was difficult to suggest the exact structure of probable catalyst-substrate aggregate from ESI-MS. Further, in order to understand more, the qualitative detection of H₂O₂ during the catalytic procedure was monitored by observing the band at 353 nm, which correspond to formation of I₃⁻ using UV-Vis spectroscopy. The results obtained suggest oxidation of I to I2 and subsequent formation of I₃ which was found using UV-Vis spectroscopy. It clearly indicates the liberation of hydrogen peroxide through reduction of molecular aerial oxygen [83]. So, from the above details, mechanistic route (Scheme 4.5) for catalytic oxidation of 2aminophenol is proposed in which catalytic oxidation occurs through oaminophenol bound active species of trinuclear Zn(II) complex and subsequent coupling (dimerization) of o-quinone imine to give phenoxazinone [89].

$$\begin{array}{c} \begin{array}{c} \begin{array}{c} \begin{array}{c} \begin{array}{c} \\ \\ \\ \\ \end{array} \end{array} \end{array} \begin{array}{c} \begin{array}{c} \\ \\ \\ \end{array} \end{array} \begin{array}{c} \\ \\ \end{array} \end{array} \begin{array}{c} \\ \\ \\ \end{array} \begin{array}{c} \\ \\ \end{array} \end{array} \begin{array}{c} \\ \\ \\ \end{array} \begin{array}{c} \\ \\ \\ \end{array} \begin{array}{c} \\ \\ \end{array} \begin{array}{c} \\ \\ \end{array} \begin{array}{c} \\ \\ \\ \\ \end{array} \begin{array}{c} \\ \\ \\ \end{array} \begin{array}{c} \\ \\ \\ \\ \end{array} \begin{array}{c} \\ \\ \\ \\ \end{array} \begin{array}{c} \\ \\ \\ \end{array} \begin{array}{c} \\ \\ \\ \\ \\ \end{array} \begin{array}{c} \\ \\ \\ \\ \end{array} \begin{array}{c} \\ \\ \\ \\ \\ \end{array} \begin{array}{c} \\ \\ \\ \\ \\ \end{array} \begin{array}{c} \\ \\ \\ \\ \\ \\ \end{array} \begin{array}{c} \\ \\ \\ \\ \\ \end{array} \begin{array}{c} \\ \\ \\ \\ \\ \\ \end{array} \begin{array}{c} \\ \\ \\ \\ \\ \\ \end{array} \begin{array}{c} \\ \\ \\ \\ \\ \end{array} \begin{array}{c}$$

Scheme 4.5: Probable mechanistic route for catalytic conversion of 2-AP by zinc(II) complex

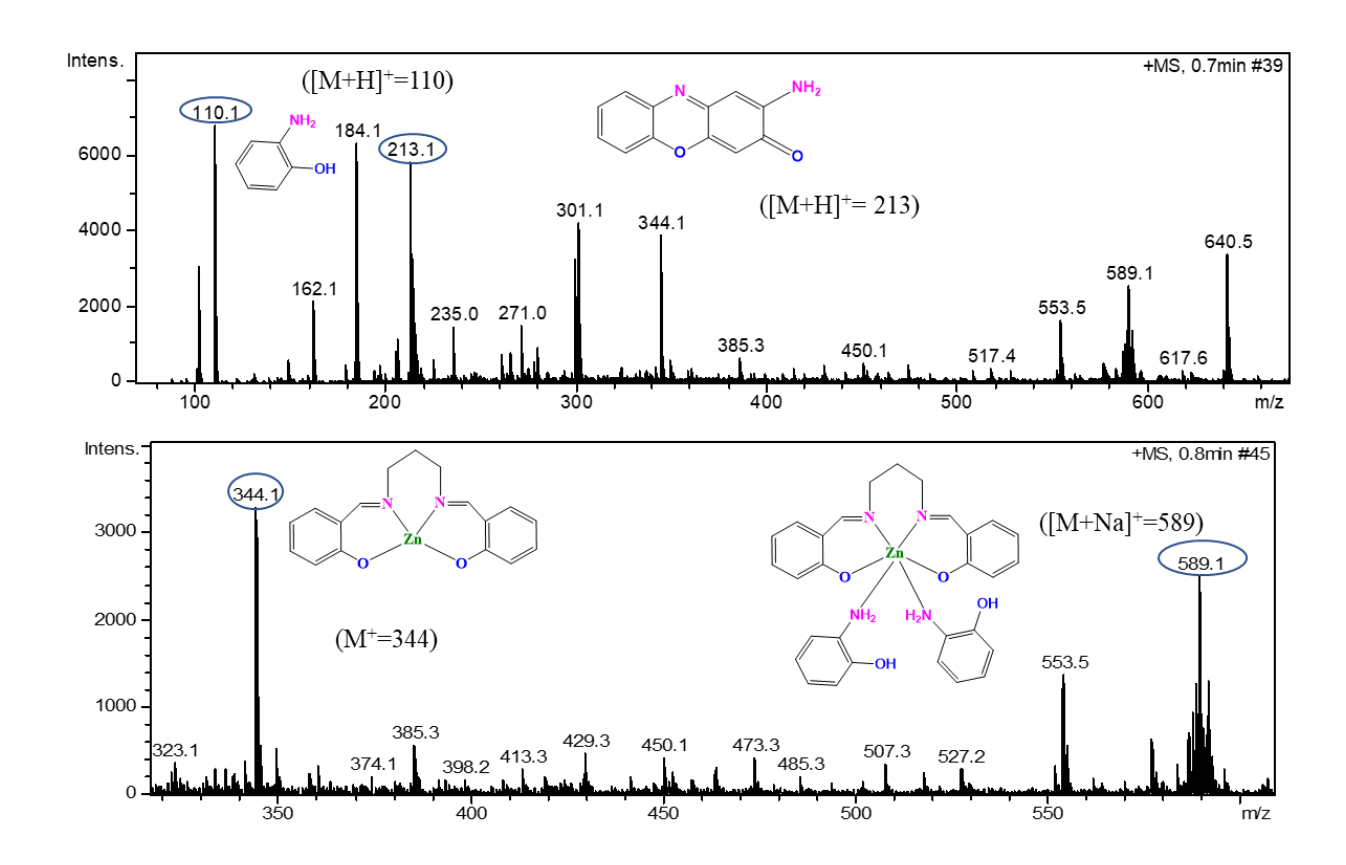


Figure 4.18: ESI-MS spectrum recorded within 20 minutes of the oxidation reaction

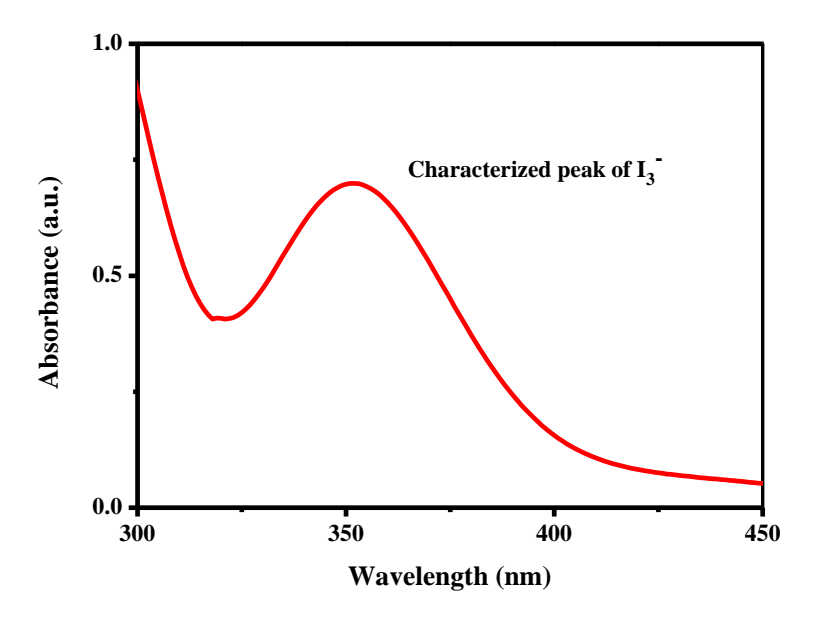


Figure 4.19: Characterized peak of I₃⁻ for the qualitative detection of H₂O₂ in **1** during the catalytic oxidation process

4.3 BSA Binding study

To examine the binding ability of nickel complexes with BSA protein, fluorescence quenching studies has been analyzed. For this purpose, quenching experimentations were done using the solution of BSA in presence of an increasing concentration of the different complexes 2 and 3. Significant decrease in intensity of the fluorophore (Figure 4.20-2.21) indicates the probable interactions between the complexes and the protein solution.

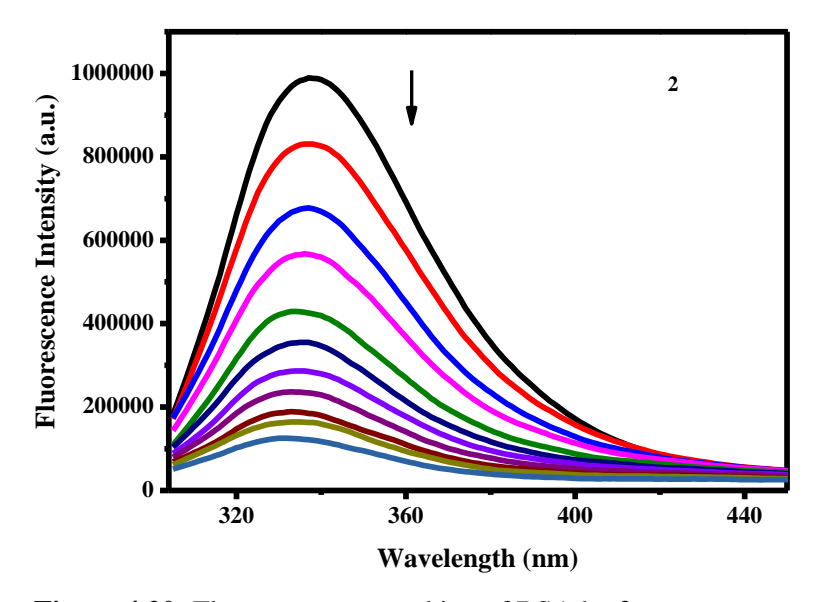


Figure 4.20: Fluorescence quenching of BSA by 2

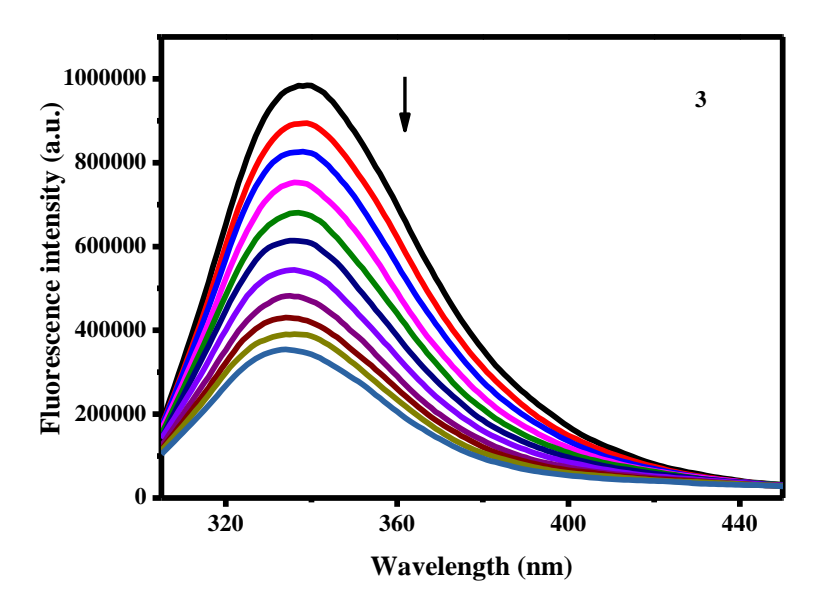


Figure 4.21: Fluorescence quenching of BSA by 3

To get more understanding into the quenching procedure, obtained fluorescence quenching data was studied using **Stern-Volmer equation** (graphs are shown in figure 4.22 - 4.23)

$$\frac{F_0}{F} = 1 + K_q \tau_o [Q] = 1 + K_{sv} [Q]$$

Q = Concentration of Quencher, τ_0 = Average life time in absence of Q

F = Fluorescence intensity in presence of quencher

 F_0 = Fluorescence intensity in absence of quencher

 $K_{SV} = Stern-Volmer$ quenching constant

 $K_q = Bimolecular \ quenching \ rate \ constant$

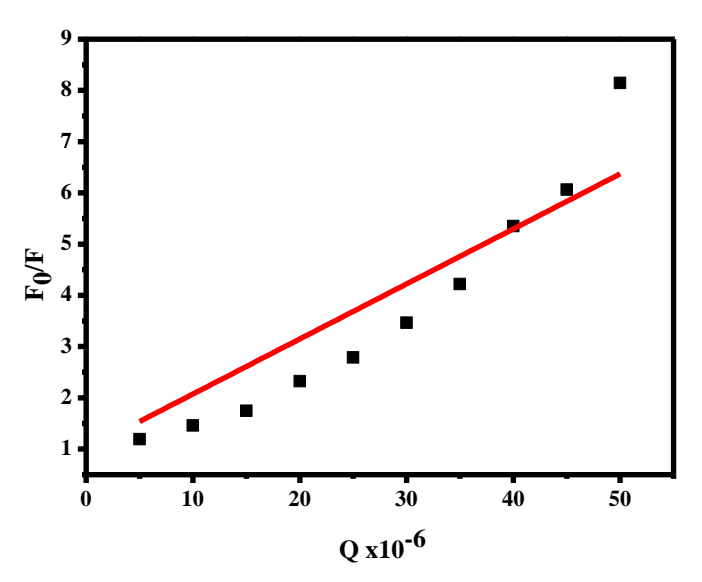


Figure 4.22: Stern -Volmer plot for 2

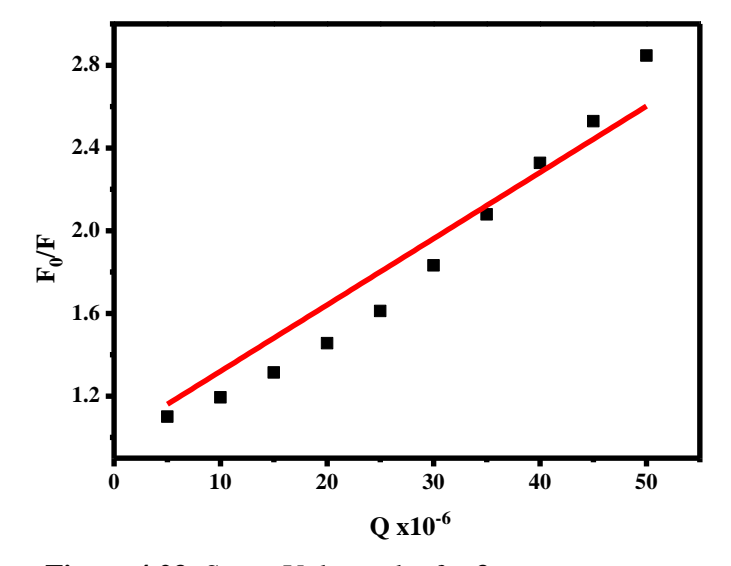


Figure 4.23: Stern -Volmer plot for 3

Scathard equation is used to determine the value of n and K_a , according to which,

$$\log \left[\frac{F_0 - F}{F} \right] = \log K_a + n \log [Q]$$

 $K_a = Binding constant$

n = Number of binding sites.

Therefore, graph between log $[(F_0 - F)/F]$ on y-axis $vs \log[Q]$ on x-axis (graphs are shown in figure 4.24 - 4.25) is plotted to determine the value of n (slope) and the value of K_a (intercept).

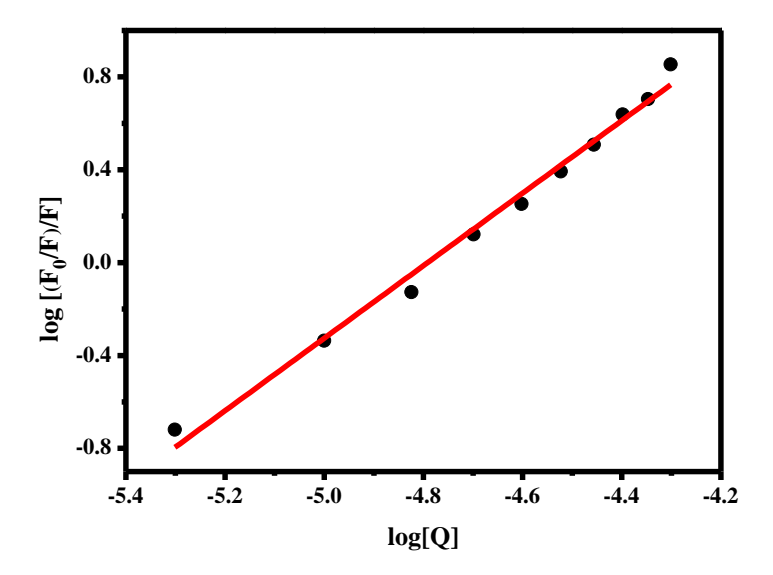


Figure 4.24: Scatchard plot for 2

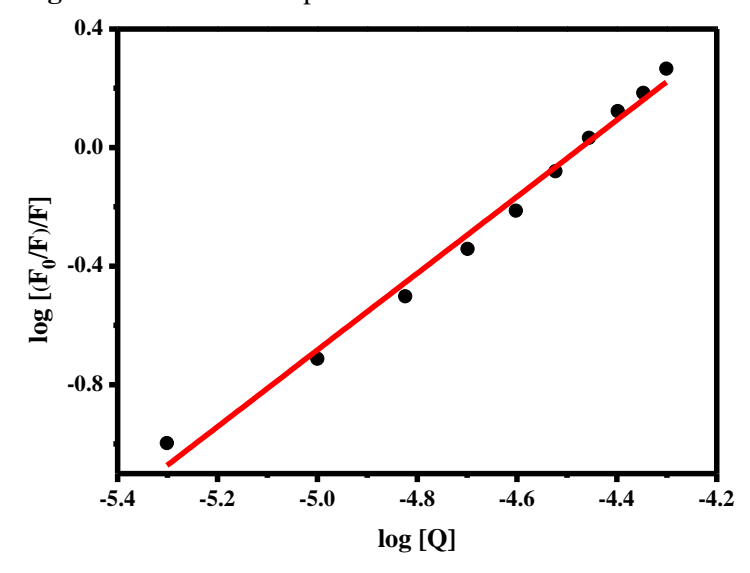


Figure 4.25: Scatchard plot for 3

4.4 HSA binding study

To examine the binding ability of nickel complexes with HSA protein, fluorescence quenching studies has been analyzed. For this purpose, quenching experimentations were done using the solution of HSA in presence of an increasing concentration of the different complexes $\mathbf{2}$ and $\mathbf{3}$. Significant decrease in intensity of the fluorophore indicates the probable interactions (figure 4.26 - 4.27).

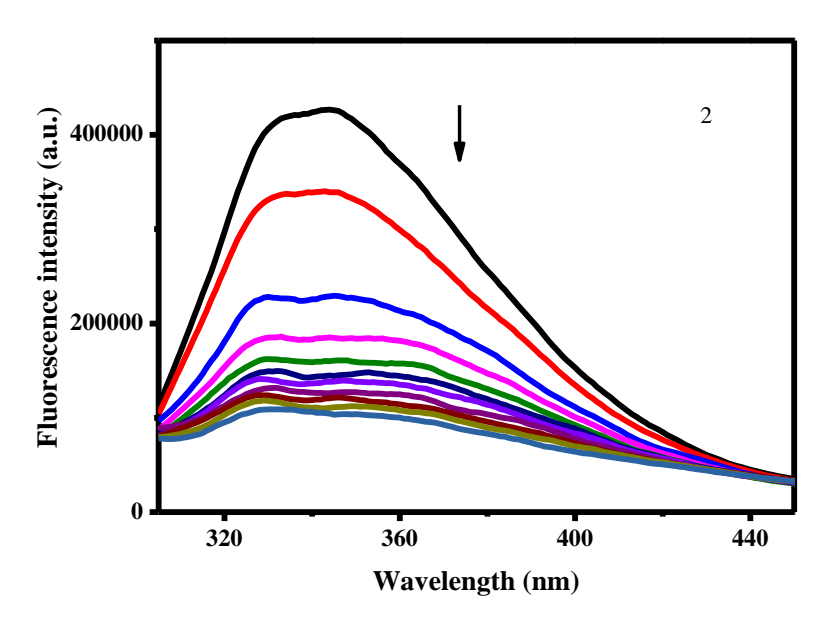


Figure 4.26: Fluorescence quenching of HSA by 2

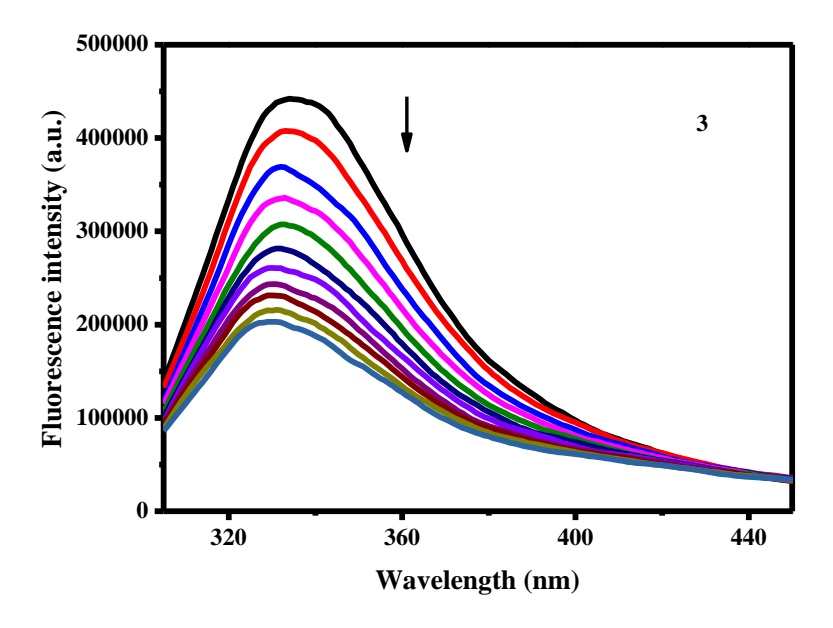


Figure 4.27: Fluorescence quenching of HSA by 3

Fluorescence quenching data obtained was studied using **Stern-Volmer equation** (graphs shown in Figure 4.28 - 4.29).

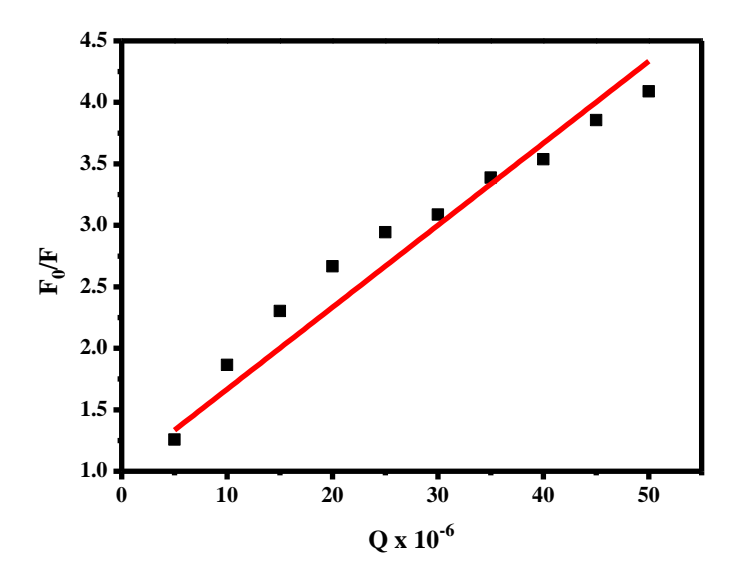


Figure 4.28: Stern-Volmer plot for 2

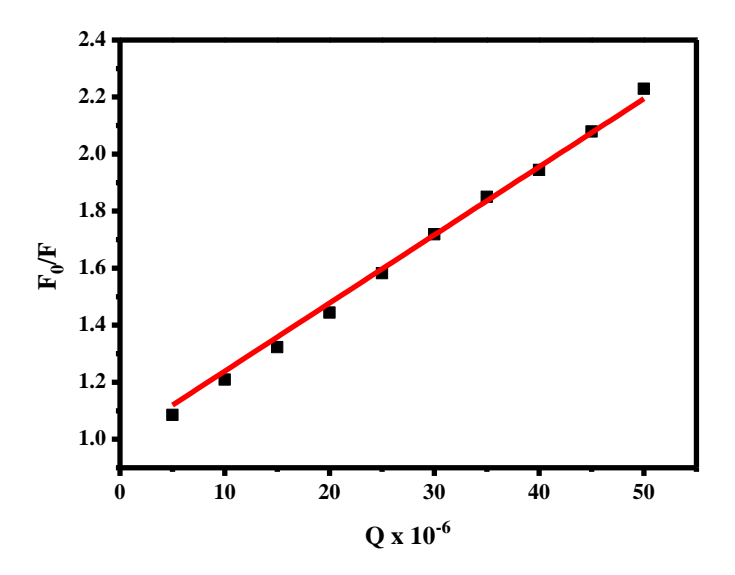


Figure 4.29: Stern-Volmer plot for 3

Scatchard plot (Figure 4.30 $-\,4.31)$ was drawn to determine the value of K_a and n.

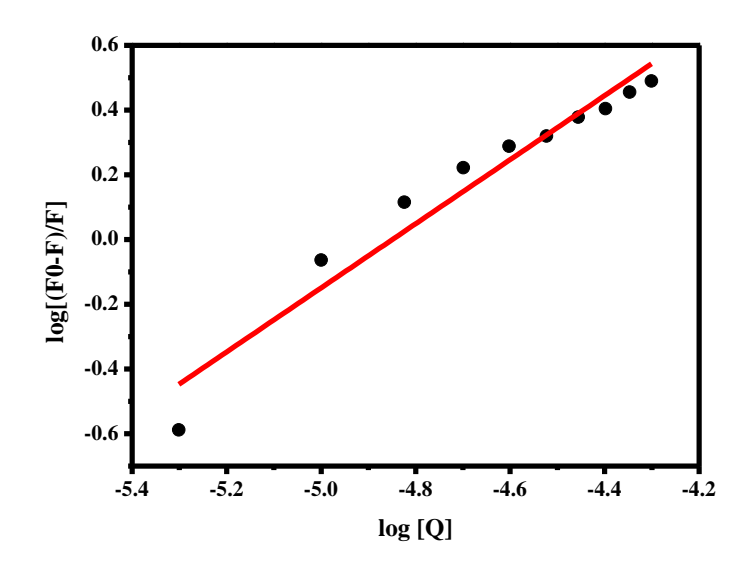


Figure 4.30: Scatchard plot for 2

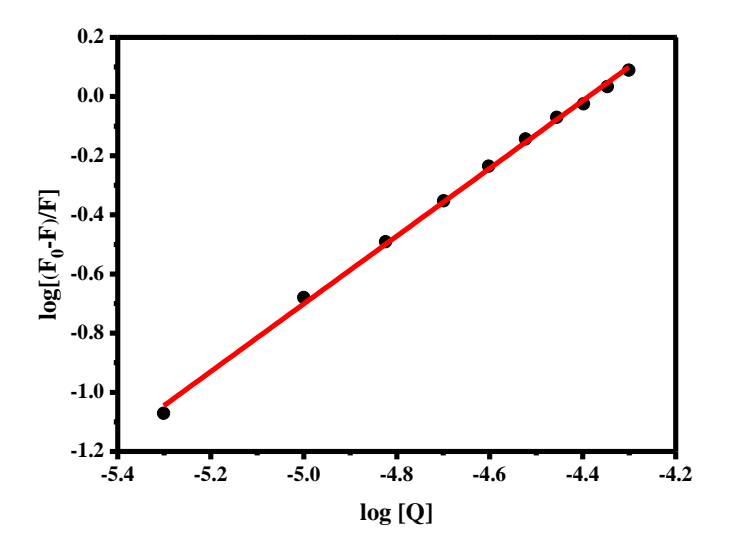


Figure 4.31: Scatchard plot for 3

The values calculated using Stern-Volmer equation and Scatchard equation of K_{sv} , K_q , K_a and n for the binding affinity of the nickel complexes with the proteins are shown in Table 4.11 indicating substantial HSA and BSA binding ability of the complexes.

Table 4.11: Table showing the value of $K_{\mbox{\scriptsize sv}},\,K_{\mbox{\scriptsize q}},\,K_{\mbox{\scriptsize a}}$ and n

Complex	K _{SV} (M ⁻¹)	$K_q (M^{-1} s^{-1})$	K _a (M ⁻¹)	n
2 (BSA)	1.07×10^5	1.73×10^{13}	3.04×10^{7}	1.56
2 (HSA)	6.67×10^4	1.07×10^{13}	6.30×10^4	0.99
3 (BSA)	3.20×10^4	5.17×10^{12}	6.07×10^5	1.29
3 (HSA)	2.38×10^{4}	3.85×10^{12}	1.05×10^5	1.14

Chapter 5

Conclusion and Future Scope

In the present work, three new trinuclear complexes (1-3) based on " N_2O_2 " donor (salen type) symmetrical dicondensed Schiff base ligand have been synthesized successfully. Trinuclear Zn(II) complex (1) shows high catalytic activity towards phenoxazinone synthase, which is found to be more than the previously reported zinc complex analogue [74]. H_2O_2 was detected during the oxidation of 2-aminophenol to phenoxazinone.

Both the trinuclear nickel tetrazolato complexes (2 and 3) showed significant protein binding activity when examined using BSA and HSA proteins. The results show that Schiff base ligands with "N₂O₂" donor set can form interesting metal complexes which exhibit suitable biometric properties that can mimic the active sites and can show a high affinity towards protein binding. In the future, various metal complexes with different co-ligands can be synthesized and explored for different applications.

REFERENCES

- [1] Constable E.C., Housecroft C.E. (2013), Coordination chemistry: the scientific legacy of Alfred Werner, Chem Soc Rev, 42, 1429-1439. (DOI:10.1039/C2CS35428D)
- [2] Kauffman G.B. (1994), Theories of Coordination Compounds and Coordination Chemistry, J Am Chem Soc, 2–33. (DOI: 10.1021/bk-1994-0565.ch001)
- [3] Gupta 1.K., Sutar A.K. (2008), Catalytic activities of Schiff base transition metal complexes, Coord Chem Rev, 252, 1420-1450. (DOI: 10.1016/j.ccr.2007.09.005)
- [4] Biswas B., Al-Hunaiti A., Räisänen M. T., Ansaloni S., Leskelä M., Repo T., Garcia Y. (2012), Efficient and selective oxidation of primary and secondary alcohols using an iron (III)/phenanthroline complex: structural studies and catalytic activity, Eur J Inorg Chem, 2012, 4479-4485. (DOI: 10.1002/ejic.201200658)
- [5] Peng Y., Singh M.K., Mereacre V., Anson C., Rajaraman G., Powell A. K. (2019), Mechanism of Magnetization Relaxation in {MIII2DyIII2} (M= Cr, Mn, Fe, Al) "Butterfly" Complexes: How Important Are the Transition Metal Ions Here?, Chem Sci, 10, 5528-5538. (DOI:10.1039/C8SC05362F)
- [6] Xue X., Wang H., Han Y., Hou H. (2018), Photoswitchable nonlinear optical properties of metal complexes, Dalton Trans, 47, 13-22. (DOI:10.1039/C7DT03989A)
- [7] Hinaly B., et al. (2018), J Chem & Cheml Sci, 8, 595-605. (DOI-10.29055/jccs/614)

- [8] Datta S., Saha M.L., Stang P.J. (2018), Hierarchical assemblies of supramolecular coordination complexes, Acc Chem Res, 51, 2047-2063. (DOI: 10.1021/acs.accounts.8b00233)
- [9] Lorenzini C., Pelizzi C., Pelizzi G., Predieri G. (1983), Investigation into aroylhydrazones as chelating agents. Part 4. Synthesis and spectroscopic characterization of Co II, Ni II, Cu II, and Zn II complexes of 2, 6-diacetylpyridine bis (2-thenoylhydrazone) and X-ray crystal structure of bis [2, 6-diacetylpyridine bis (2-thenoylhydrazonato) (2–)] dizinc (II), J Chem Soc, Dalton Trans, (10), 2155-2158.

 (DOI: 10.1039/DT9830002155)
- [10] Rodrìguez-Argüelles M.C., Ferrari M.B., Bisceglie F., Pelizzi C., Pelosi G., Pinelli S., Sassi M. (2004), Synthesis, characterization and biological activity of Ni, Cu and Zn complexes of isatinhydrazones, J Inorg Biochem, 98, 313-321.(DOI: 10.1016/j.jinorgbio.2003.10.006)
- [11] Yousif E., Majeed A., Al-Sammarrae K., Salih N., Salimon J. Abdullah B. (2017), Metal complexes of Schiff base: Preparation, characterization and antibacterial activity, Arabian J Chem, 10, S1639–44. (DOI:10.1016/j.arabjc.2013.06.006)
- [12] Nejo A.A., Kolawole G.A., Nejo A.O. (2010), Synthesis, characterization, antibacterial, and thermal studies of unsymmetrical Schiff-base complexes of cobalt (II), J Coord Chem, 63, 4398-4410. (DOI:10.1080/00958972.2010.532871)
- [13] Nagesh G.Y., Mruthyunjayaswamy B.H.M. (2015), Synthesis, characterization and biological relevance of some metal (II) complexes with oxygen, nitrogen and oxygen (ONO) donor Schiff base ligand derived from thiazole and 2-hydroxy-1-naphthaldehyde, J Mol Struct, 1085, 198-206. (DOI: 10.1016/j.molstruc.2014.12.058)

- [14] Refat M.S., El-Sayed M.Y., Adam A.M.A. (2013), Cu (II), Co (II) and Ni (II) complexes of new Schiff base ligand: synthesis, thermal and spectroscopic characterizations, J Mol Struct, 1038, 62-72. (DOI: 10.1016/j.molstruc.2013.01.059)
- [15] Lo, K.K.W. (Ed.). (2016), Inorganic and organometallic transition metal complexes with biological molecules and living cells, first ed., Academic Press, pp. 406 (ISBN).
- [16] Petoud S., Cohen S.M., Bünzli J.C.G., Raymond K.N. (2003), Stable lanthanide luminescence agents highly emissive in aqueous solution: multidentate 2-hydroxyisophthalamide complexes of Sm³⁺, Eu³⁺, Tb³⁺, Dy³⁺, J Am Chem Soc, 125, 13324-13325.

 (DOI:10.1021/ja0379363)
- [17] Dau H., Haumann M. (2008), The manganese complex of photosystem II in its reaction cycle—basic framework and possible realization at the atomic level, Coord Chem Rev, 252, 273-295.

 (DOI: 10.1016/j.ccr.2007.09.001)
- [18] Stohs S.J., Bagchi D. (1995), Oxidative mechanisms in the toxicity of metal ions, Free radical Bio Med, 18, 321-336. (DOI:10.1016/0891-5849(94)00159-h)
- [19] Carter K.P., Young A.M., Palmer A.E. (2014), Fluorescent sensors for measuring metal ions in living systems, Chem Rev, 114, 4564-4601. (DOI:10.1021/cr400546e)
- [20] Wilkinson S.M., Sheedy T.M., New E.J. (2015), Synthesis and characterization of metal complexes with Schiff base ligands, J Chem Educ, 93, 351-354. (DOI: 10.1021/acs.jchemed.5b00555)
- [21] Shaygan S., Pasdar H., Foroughifa, N., Davallo M., Motiee F. (2018),Cobalt (II) Complexes with Schiff Base Ligands Derived from

- Terephthalaldehyde and ortho-Substituted Anilines: Synthesis, Characterization and Antibacterial Activity, Appl Sci, 8, 385. (DOI:10.3390/app8030385)
- [22] Klapötke T.M., Sabaté C.M., Stierstorfer J. (2009), Neutral 5-nitrotetrazoles: easy initiation with low pollution, New J Chem, 33, 136–47. (DOI: 10.1039/B812529E)
- [23] Evenyl L, Rosen C. (2009), Redox active N-Heterocyclic carbenes:design synthesis and evaluation of their electronic properties, Organometallics, 28, 6695-6706. (DOI: 10.1021/om900698x)
- [24] Mihina J.S., HERBST R.M. (1950), The reaction of nitriles with hydrazoic acid: Synthesis of monosubstituted tetrazoles, J Org Chem, 15, 1082-1092. (DOI:10.1021/jo01151a027)
- [25] Ostrovskii V.A., Trifonov R.E., Popova E.A. (2012), Medicinal chemistry of tetrazoles, Russ Chem Bull, 61, 768-780. (DOI:10.1016/s0079-6468(08)70159-0)
- [26] Hansch C., Leo A., Hoekman D.H. (1995), Exploring QSAR: fundamentals and applications in chemistry and biology (Vol. 557), Washington, DC, American Chemical Society. (DOI:10.1021/bk-1995-0606.ch019)
- [27] Zhao, T. (2016), Novel Application of Tetrazoles Derived from the TMSN3-Ugi Reaction, Rijksuniversiteit Groningen.
- [28] Zhao H., Qu Z.R., Ye H.Y., Xiong R.G. (2008), In situ hydrothermal synthesis of tetrazole coordination polymers with interesting physical properties, Chem Soc Rev, 37, 84-100. (DOI: 10.1039/b616738c)

- [29] Liu Y.Q., Ren G.J., Zhang Y.H., Xu J., Bu X.H. (2015), Constructing novel Cd (ii) metal—organic frameworks based on different highly connected secondary building units via alteration of reaction conditions, Dalton Trans, 44, 20361-20366. (DOI: 10.1039/C5DT02987B)
- [30] Meng G.X., Feng Y.M., Wang Y., Gao Y.L., Wan W.W., Huang X.T. (2015), Effect of pH on the self-assembly of three Cd (II) coordination compounds containing 5-(4-pyridyl) tetrazole: Syntheses, structures, and properties, J Coord Chem, 68, 1705-1718.

 (DOI:10.1080/00958972.2015.1024668)
- [31] Malviya N., Mandal P., Das M., Ganguly R., Mukhopadhyay S. (2017), Nickel tetrazolato complexes synthesized by microwave irradiation: Catecholase like activity and interaction with biomolecules, J Coord Chem, 70, 261-278. (DOI: 10.1080/00958972.2016.1260121)
- [32] Pham T., Forrest K.A., Hogan A., McLaughlin K., Belof J.L., Eckert J., Space B. (2014), Simulations of hydrogen sorption in rht-MOF-1: Identifying the binding sites through explicit polarization and quantum rotation calculations, J Mater Chem A, 2, 2088-2100. (DOI: 10.1039/C3TA14591C)
- [33] Wriedt M., Sculley J.P., Yakovenko A.A., Ma Y., Halder G.J., Balbuena P.B., Zhou H.C. (2012), Low-Energy Selective Capture of Carbon Dioxide by a Pre-designed Elastic Single-Molecule Trap, Angew Chem Int Ed, 51, 9804-9808. (DOI:10.1002/anie.201202992)
- [34] Chohan Z.H., Supuran C.T., Scozzafava A. (2004), Metalloantibiotics: synthesis and antibacterial activity of cobalt (II), copper (II), nickel (II) and zinc (II) complexes of kefzol, J Enzyme Inhib Med Chem, 19, 79-84. (DOI:10.1080/14756360310001624939)
- [35] Ren G.J., Han S.D., Liu Y.Q., Hu T.L., Bu X.H. (2016), Two Six-Connected MOFs with Distinct Architecture: Synthesis, Structure,

- Adsorption, and Magnetic Properties, ChemPlusChem, 81, 775-779. (DOI:10.1002/cplu.201600092)
- [36] Wriedt M., Yakovenko A.A., Halder G.J., Prosvirin A.V., Dunbar K.R., Zhou H.C. (2013), Reversible switching from antiferro-to ferromagnetic behavior by solvent-mediated, thermally-induced phase transitions in a trimorphic MOF-based magnetic sponge system, J Am Chem Soc, 135, 4040-4050. (DOI:10.1021/ja312347p)
- [37] Yang E.C., Liu Z.Y., Wu X.Y., Chang H., Wang E.C., Zhao X. J. (2011), Co II, Mn II and Cu II-directed coordination polymers with mixed tetrazolate–dicarboxylate heterobridges exhibiting spin-canted, spin-frustrated antiferromagnetism and a slight spin-flop transition, Dalton Trans, 40, 10082-10089. (DOI: 10.1039/C1DT10958H)
- [38] Hou Z.J., Liu Z.Y., Liu N., Yang E.C., Zhao X.J. (2015), Four tetrazolate-based 3D frameworks with diverse subunits directed by inorganic anions and azido coligand: hydro/solvothermal syntheses, crystal structures, and magnetic properties, Dalton Trans, 44, 2223-2233. (DOI: 10.1039/C4DT03172E)
- [39] Liu D.S., Chen W.T., Huang J.G., Cheng X.D., Wang J., Sui Y. (2016), Syntheses, structures and investigation of the properties of mercury coordination polymers based on 5-amino-tetrazolate ligands, CrystEng Comm, 18,7865-7872. (DOI: 10.1039/C6CE01790H)
- [40] Chen H.F., Yang W.B., Lin L., Guo X.G., Dui X.J., Wu X.Y., Zhang C. J. (2013), Cadmium (II) and Copper (II) coordination polymers based on 5-(Pyrazinyl) tetrazolate ligand: Structure, photoluminescence, theoretical calculations and magnetism, J Solid State Chem, 201, 215-221. (DOI: 10.1016/j.jssc.2013.02.038)

- [41] Bergmann L., Friedrichs J., Mydlak M., Baumann T., Nieger M., Bräse S. (2013), Outstanding luminescence from neutral copper (I) complexes with pyridyl-tetrazolate and phosphine ligands, Chem Commun, 49, 6501-6503. (DOI: 10.1039/C3CC42280A)
- [42] Saha M., Das M., Nasani R., Choudhuri I., Yousufuddin M., Nayek H. P., Mukhopadhyay S. (2015), Targeted water soluble copper–tetrazolate complexes: interactions with biomolecules and catecholase like activities, Dalton Trans, 44, 2015420167.
 (DOI: 10.1039/C5DT01471A)
- [43] Yang J. (2016), Mono-and dinuclear palladium (ii) complexes containing both N-heterocyclic carbenes and tetrazole ligands as catalysts for Hiyama coupling, New J Chem, 40, 9739-9745. (DOI: 10.1039/C6NJ02320G)
- [44] Mukhopadhyay S., Mukhopadhyay B.G., Silva M.F.C.G.D., Lasri J., Charmier M.A.J., Pombeiro A.J. (2008), PtII-Promoted [2+ 3] Cycloaddition of Azide to Cyanopyridines: Convenient Tool toward Heterometallic Structures, Inorg Chem, 47, 11334-11341. (DOI:10.1021/ic8014223)
- [45] Bhattacharya S., Roy S., Chattopadhyay S. (2016), Tetrazolate bridged dinuclear photo-luminescent zinc (II) Schiff base complex prepared via 1, 3-dipolar cycloaddition at ambient condition, J Coord Chem, 69, 915-925. (DOI:10.1080/00958972.2016.1153078)
- [46] Zhong D.C., Wen Y.Q., Deng J.H., Luo X.Z., Gong Y.N., Lu T.B. (2015), Uncovering the role of metal catalysis in tetrazole formation by an in-situ cycloaddition reaction: an experimental approach, Angew Chem Int Ed, 54, 11795-11799. (DOI:10.1002/anie.201505118)

- [47] Schiff H. (1864), Mittheilungenaus dem Universitätslaboratorium in Pisa: eineneueReiheorganischerBasen, Justus LiebigsAnnalen der Chemie, 131, 118-119. (DOI: 10.1002/jlac.18641310113)
- [48] Baldaniya B.B., Patel P.K. (2009), Synthesis, Antibacterial and Antifungal Activities of s Derivatives, Journal of Chemistry, 6, 673-680. (DOI:10.1155/2009/196309)
- [49] Angélica de Fátima S.B., Andrade C.K.Z. (2019), Synthesis of (macro) heterocycles by consecutive/repetitive isocyanide-based multicomponent reactions, Beilstein J Org Chem, 15, 906-930. (DOI:10.3762/bjoc.15.88)
- [50] Bhatt, U. (2011), Five-Membered Heterocycles with Four Heteroatoms: Tetrazoles, Modern Heterocyclic Chemistry, 1401-1430.(DOI:10.1002/9783527637737.ch15)
- [51] Bladin, J.A. (1885), Ueber von Dicyanphenylhydrazin abgeleitete Verbindungen. Berichte Der Deutschen Chemischen Gesellschaft, 18, 1544–51. (DOI: 10.1002/cber.188501801335)
- [52] Demko Z.P., Sharpless K.B. (2001), Preparation of 5-substituted 1 H-tetrazoles from nitriles in water, J Org Chem, 66, 7945-7950. (DOI:10.1021/jo010635w)
- [53] Venkateshwarlu G., Premalatha A., Rajanna K.C. Saiprakash P.K. (2009), Cadmium Chloride as an Efficient Catalyst for Neat Synthesis of 5-Substituted 1H-Tetrazoles, Synth Commun, 39, 4479–85. (DOI:10.1080/00397910902917682)
- [54] Lakshmi Kantam M., Balasubrahmanyam V., Kumar K.S. (2006), Zinc Hydroxyapatite—Catalyzed Efficient Synthesis of 5-Substituted 1 H-Tetrazoles, Synth Commun, 36, 1809-1814.
 (DOI: 10.1080/00397910600619630)

- [55] Amantini D, Bellegia R (2004), TBAF-Catalyzed Synthesis of 5-Substituted 1H-Tetrazoles under Solventless Conditions, J Org, 69, 2896-2898. (DOI:10.1021/jo0499468)
- [56] Bonnamour J., Bolm C. (2009), Iron Salts in the Catalyzed Synthesis of5-Substituted 1H-Tetrazoles, Chem Eur J, 15, 4543–5.(DOI: 10.1002/chem.200900169)
- [57] Muthusami R., Moorthy M., Irena K., Govindaraj A., Manickam C., Rangappan R. (2018), Designing a biomimetic catalyst forphenoxazinone synthase activity using a mesoporous Schiff base copper complex with a novel double-helix morphology, New J Chem, 42, 18608-18620. (DOI:10.1039/C8NJ03638A)
- [58] Dey S.K., Mukherjee A. (2013), Zero-Order Catechol Oxidase Activity by a Mononuclear Manganese (III) Complex Showing High Turnover Comparable to Catechol Oxidase Enzyme, ChemCatChem, 5, 3533-3537. (DOI: 10.1002/cctc.201300596)
- [59] Que Jr L., Ho R.Y. (1996), Dioxygen activation by enzymes with mononuclear non-heme iron active sites, Chem Rev, 96, 2607-2624. (DOI:10.1021/cr960039f)
- [60] Merkel M., Pascaly M., Krebs B., Astner J., Foxon S. P., Schindle S. (2005), Chelate ring size variations and their effects on coordination chemistry and catechol dioxygenase reactivity of iron (III) complexes, Inorg Chem, 44, 7582-7589. (DOI:10.1021/ic050708k)
- [61] Suzuki M., Furutachi H., Ōkawa H. (2000), Bimetallic dioxygen complexes derived from 'end-off' compartmental ligands, Coord Chem Rev, 105-129. (DOI:10.1016/s0010-8545(00)00323-4)

- [62] Lyons C.T., Daniel T., Stack P. (2013), The challenge of cyclic and acyclic schiff bases and related derivatives, Coord Chem Rev, 257, 528-540.
- [63] Smith A.W., Camara-Artigas A., Wang M., Allen J.P., Francisco W.A. (2006), Structure of phenoxazinone synthase from Streptomyces antibioticus reveals a new type 2 copper center, Biochemistry, 45, 4378-4387. (DOI:10.1021/bi0525526)
- [64] Carter D.C., Ho J.X. (1994), Structure of serum albumin, Advances in protein chemistry (Vol. 45), Academic Press, pp. 153-203.(DOI:10.1016/s0065-3233(08)60640-3)
- [65] Kosa T., Maruyama T., Otagiri M. (1997), Species differences of serum albumins: I. Drug binding sites, Pharm Res, 14, 1607-1612.(DOI:10.1023/a:1012138604016)
- [66] Moreno F., Cortijo M., González-Jiménez J. (1999), The fluorescent probe prodan characterizes the warfarin binding site on human serum albumin, Photochem Photobiol, 69, 8-15.

 (DOI:10.1111/j.1751-1097. 1999.tb05299.x)
- [67] Peters, Jr T. (1985), Serum albumin, Advances in protein chemistry (Vol. 37), Academic Press, pp. 161-245.(DOI:10.1016/s0065-3233(08)60065-0)
- [68] He X.M., Carter D.C. (1992), Atomic structure and chemistry of human serum albumin, Nature, 358, 209. (DOI:10.1038/358209a0)
- [69] Belatik A., Hotchandani S., Carpentier R., Tajmir-Riahi H.A. (2012), Locating the binding sites of Pb (II) ion with human and bovine serum albumins, PLoS One, 7, e36723.

 (DOI: 10.1371/journal.pone.0036723)

- [70] Vigato P.A., Tamburini S. (2004), The challenge of cyclic and acyclic Schiff bases and related derivatives, Coord Chem Rev, 248, 1717-2128. (DOI: 10.1016/j.cct.2003.09.003)
- [71] Hazari A., Das L.K., Bauzá A., Frontera A., Ghosh A. (2016), Exploring the coordinative adaptation and molecular shapes of trinuclear Cu II 2
 M II (M= Zn/Cd) complexes derived from salen type Schiff bases: structural and theoretical studies, Dalton Trans, 45, 5730-5740. (DOI: 10.1039/C5DT04941E)
- [72] Das M., Chatterjee S., Harms K., Mondal T. K., Chattopadhyay S. (2014), Formation of bis (μ-tetrazolato) dinickel (II) complexes with N, N, O-donor Schiff bases via in situ 1, 3-dipolar cyclo-additions: isolation of a novel bi-cyclic trinuclear nickel (II)–sodium (I)–nickel (II) complex, Dalton Trans, 43, 2936-2947. (DOI: 10.1039/C3DT52796D)
- [73] Ghosh K., Drew M.G., Chattopadhyay S. (2018), Synthesis and structure of a cobalt (III) complex containing pendant Schiff base ligand: Exploration of its catechol oxidase and phenoxazinone synthase like activity, Inorganica Chim Acta, 482, 23-33.

 (DOI: 10.1016/j.ica.2018.05.025)
- [74] Garai M., Das A., Joshi M., Paul S., Shit M., Choudhury A.R., Biswas B. (2018), Synthesis and spectroscopic characterization of a photostable tetrazinc (II)—Schiff base cluster: A rare case of ligand centric phenoxazinone synthase activity, Polyhedron, 156, 223-230. (DOI:10.1016/j.poly.2018.09.044)
- [75] Mahapatra P., Ghosh S., Giri S., Rane V., Kadam R., Drew M. G., Ghosh, A. (2017), Subtle Structural Changes in (CuIIL) 2MnII Complexes to Induce Heterometallic Cooperative Catalytic Oxidase Activities on Phenolic Substrates (H₂L= Salen Type Unsymmetrical Schiff Base), Inorg Chem, 56, 5105-5121.

(DOI: 10.1021/acs.inorgchem.7b00253)

- [76] Saha M., Malviya N., Das M., Choudhuri I., Mobin S.M., Pathak B., Mukhopadhyay S. (2017), Effect on catecholase activity and interaction with biomolecules of metal complexes containing differently tuned 5-substituted ancillary tetrazolato ligands, Polyhedron, 121, 155-171. (DOI:10.1016/j.poly.2016.09.035)
- [77] Saha M., Nasani R., Das M., Mahata A., Pathak B., Mobin S.M., Mukhopadhyay S. (2014), Limiting nuclearity in formation of polynuclear metal complexes through [2+3] cycloaddition: synthesis and magnetic properties of tri-and pentanuclear metal complexes, Dalton Trans, 43, 8083-8093. (DOI: 10.1039/C4DT00378K)
- [78] Tseng T.W., Luo T.T., Chen S.Y., Su C.C., Chi K.M., Lu K.L. (2012), Porous metal—organic frameworks with multiple cages based on tetrazolate ligands: synthesis, structures, photoluminescence, and gas adsorption properties, Cryst Growth Des, 13, 510-517. (DOI:10.1021/cg3009249)
- [79] Maitra U., Chakrabarty A. (2011), Protonation and deprotonation induced organo/hydrogelation: Bile acid derived gelators containing a basic side chain, Beilstein, J Org Chem, 7, 304–9.
 (DOI:10.3762/bjoc.7.40)
- [80] Hazari A., Diaz C., Ghosh A. (2018), H-bond assisted coordination bond formation in the 1D chains based on azido and phenoxido bridged tetranuclear Cu (II) complexes with reduced Schiff base ligands, Polyhedron, 142, 16-24. (DOI:10.1016/j.poly.2017.12.022)
- [81] Fatima I., Zafar H., Khan K.M., Saad S.M., Javaid S., Perveen S., Choudhary M.I. (2018), Synthesis, molecular docking and xanthine oxidase inhibitory activity of 5-aryl-1H-tetrazoles, Bioinorg Chem, 79, 201-211. (DOI: 10.1016/j.bioorg.2018.04.021)

- [82] Freeman J.C., Nayar P.G., Begley T.P., Villafranca J.J. (1993), Stoichiometry and spectroscopic identity of copper centers in phenoxazinone synthase: a new addition to the blue copper oxidase family, Biochemistry, 32, 4826-4830. (DOI:10.1021/bi00069a018)
- [83] Biswas A., Das L.K., Drew M.G., Aromí G., Gamez, P., Ghosh, A. (2012), Synthesis, crystal structures, magnetic properties and catecholase activity of double phenoxido-bridged penta-coordinated dinuclear nickel (II) complexes derived from reduced Schiff-base ligands: mechanistic inference of catecholase activity, Inorg Chem, 51, 7993-8001. (DOI:10.1021/ic202748m)
- [84] Atakol O., Nazir H., Aksu M., Anci C., Ercan F., Çiçek B. (2000), Some di-and trinuclear zinc complexes: Anion induced complex formation, Synth React Inorg M, 30, 709-718.
 (DOI: 10.1080/00945710009351793)
- [85] Simándi T.M., Simándi L.I., Győr M., Rockenbauer A., Gömöry Á. (2004), Kinetics and mechanism of the ferroxime (II)-catalysed biomimetic oxidation of 2-aminophenol by dioxygen. A functional phenoxazinone synthase model, Dalton Trans, (7), 1056-1060. (DOI: 10.1039/B316543D)
- [86] Kumar S.C., Ghosh A.K., Chen J.D., Ghosh R. (2017), Structurally characterized mononuclear Mn (II) complex: Functional model for catecholase and phenoxazinone synthase activities, Inorganica Chim Acta, 464, 49-54. (DOI: 10.1016/j.ica.2017.04.043)
- [87] Balakrishnan C., Neelakantan M.A. (2018), Crystal structure and biocatalytic potential of oxovanadium (IV) Schiff base complexes derived from 2-hydroxy-4-(prop-2-yn-1-yloxy) benzaldehyde and alicyclic/aromatic diamines, Inorganica Chim Acta, 469, 503-514. (DOI: 10.1016/j.ica.2017.09.060)

- [88] Mahato M., Van Hecke K., Nayek H.P. (2018), Two mononuclear cobalt (III) complexes exhibiting phenoxazinone synthase activity, Appl Organomet Chem, 32, e4336. (DOI:10.1002/aoc.4336)
- [89] Jana N.C., Brandão P., Bauzá A., Frontera A., Panja A. (2017), Influence of ancillary ligands on preferential geometry and biomimetic catalytic activity in manganese (III)-catecholate systems: A combined experimental and theoretical study, J Inorg Biochem, 176, 77-89. (DOI:10.1016/j.jinorgbio.2017.08.008)